Outage Analysis of Millimeter Wave RSMA Systems

Hongjiang Lei, *Senior Member, IEEE,* Sha Zhou, Ki-Hong Park, *Senior Member, IEEE,* Imran Shafique Ansari, *Member, IEEE,* Hong Tang, and Mohamed-Slim Alouini, *Fellow, IEEE*

***Abstract*—Millimeter-wave (mmWave) communication has attracted considerable attention from academia and industry, providing multi-gigabits per second rates due to the substantial bandwidth. Rate splitting multiple access (RSMA) is an effective technology that provides a generalized multiple access framework. Regarding the new propagation characteristics of the mmWave, we investigate the outage performance of the mmWave RSMA multiple-input-single-output system with a fixed-located user and a randomly-located user. Based on the spatial correlation of the paired users, the user's paths are divided into overlapped and non-overlapped paths. Two beamforming schemes are proposed to improve the reliability of the mmWave RSMA system. The common stream is transmitted on the overlapped paths or all the paths. By utilizing stochastic geometry theory, the closed-form expressions of the outage probability (OP) with proposed schemes are derived. To obtain more insights, the expressions for the asymptotic OP are derived. Monte Carlo simulation results are presented to validate the analysis and the effects of the system parameters, such as power allocation coefficients and the number of resolvable paths, on the outage performance are investigated.**

***Index Terms*—Millimeter wave, rate splitting multiple access, stochastic geometry, outage probability.**

I. Introduction

A. Background and Related Work

The popularity of various mobile smart devices has greatly stimulated challenging demands for wireless communications with respect to available bandwidth and extremely high data rates. Millimeter-wave (mmWave) communication has become one of the most efficient solutions for future wireless communication and has drawn considerable attention from both academia and industry [1], [2]. Different from rich scattering environments of the traditional low-frequency channels, the mmWave channels are characterized by sparse scattering and multipath that can be described by a geometric channel model [3]. Two random beamforming schemes were proposed for mmWave non-orthogonal multiple access (NOMA) systems to reduce feedback in [4] and the expressions for the exact and asymptotic outage probability (OP) were derived, respectively. The authors in [5] investigated the security, reliability, and energy coverage of downlink mmWave simultaneous wireless information and power transfer unmanned aerial vehicle (UAV) NOMA systems. In [6], a new mmWave-NOMA framework under geometric channel model was proposed wherein users were classified as secure users and common users.

To characterize multipath transmission of mmWave channel, Ju *et al.* in [7] utilized a discrete angular domain channel model under geometric channel model, which is more conducive in encompassing the new propagation characteristics and flexible and suitable for theoretical analysis of mmWave systems. Then, three transmission schemes were designed to enhance the secrecy performance of a multiple-input-single-output (MISO) mmWave system. The results demonstrated that the relationship between the legitimate user's and the eavesdropper's spatially resolvable paths significantly affected the secrecy performance of the mmWave system. In [8], the authors investigated the secrecy performance of mmWave systems with randomly located multiple eavesdroppers. In [9], the MISO discrete angular domain channel was extended to the multiple input multiple output channel by designing the corresponding beamforming methods. The secrecy performance of mmWave decode-and-forward relay systems in three eavesdropping scenarios was investigated. The authors in [10] investigated the secure performance of mmWave NOMA systems wherein both legitimate and illegitimate users were randomly distributed. Two transmission schemes were proposed by considering the spatial correlation between the selected legitimate users and eavesdroppers. The closed-form expressions of the SOP for different beamforming schemes were derived.

Recently, as a generalized downlink multiple-access scheme, rate splitting multiple access (RSMA) was proposed in [11]. In downlink RSMA, each message intended for users at the transmitter is split into a common and private part. All the common parts are encoded into a common stream decoded by all users and the private parts are encoded in private

Manuscript received.

This work was supported by the National Natural Science Foundation of China under Grant 61971080 and the Open Fund of the Shaanxi Key Laboratory of Information Communication Network and Security under Grant ICNS201807.

H. Lei is with the School of Communication and Information Engineering, Chongqing University of Posts and Telecommunications, Chongqing 400065, China, also with Chongqing Key Lab of Mobile Communications Technology, Chongqing 400065, China, and also with Shaanxi Key Laboratory of Information Communication Network and Security, Xi'an University of Posts and Telecommunications, Xi'an, Shaanxi 710121, China (e-mail: leihj@cqupt.edu.cn).

S. Zhou is with the School of Communication and Information Engineering, Chongqing University of Posts and Telecommunications, Chongqing 400065, China (e-mail: cquptzhous@163.com).

I. S. Ansari is with James Watt School of Engineering, University of Glasgow, Glasgow G12 8QQ, United Kingdom (e-mail: imran.ansari@glasgow.ac.uk).

H. Tang is with the School of Communication and Information Engineering, Chongqing University of Posts and Telecommunications, Chongqing 400065, China, also with Chongqing Key Lab of Mobile Communications Technology, Chongqing 400065, China (e-mail: tangh@cqupt.edu.cn).

K.-H. Park and M.-S. Alouini are with CEMSE Division, King Abdullah University of Science and Technology (KAUST), Thuwal 23955-6900, Saudi Arabia (e-mail: kihong.park@kaust.edu.sa, slim.alouini@kaust.edu.sa).

streams decoded by the corresponding users. The common and private streams are superimposed together, linearly precoded, and transmitted simultaneously. By successive interference cancellation (SIC) technology, the common stream is decoded first by treating all private signals as interference at each receiver. After the common stream is decoded and removed from the received signals, the private stream is decoded by treating other users' private signals as interference. RSMA outperforms and unifies orthogonal multiple access, NOMA, space division multiple access (SDMA), and multicasting that was first shown through optimization in [11] and analytically in [12]. As a result, RSMA represents a new multiple-access paradigm through adaptively managing inter-user interference [13]-[15]. In [16], the RSMA scheme was utilized in the UAV downlink systems and the closed-form expressions of the OP and throughput at each user were derived. In [17], the RSMA scheme was utilized in a satellite and aerial-integrated network wherein the signals for all the users and some particular users were mapped to different beamformers, respectively. An optimization problem was proposed to maximize the sum rate of the considered system. Their results verified that the proposed beamform design frameworks could enhance spectral efficiency. The secrecy performance of two-user downlink systems with untrusted users was investigated and the closed-form expressions for the OP and secrecy OP were derived in [18] and in [19]. The authors investigated the performance of a multi-cell RSMA network and derived the analytical expressions for sum rate and spectral efficiency based on stochastic geometry theory in [20]. Their results demonstrated that the power splitting ratio between common and private streams significantly impacts performance.

The uplink RSMA scheme was proposed in [21] and their result demonstrated that it could achieve the capacity region of the multiple access channels. Relative to the downlink RSMA scheme, the messages of $K-1$ users in uplink RSMA systems with K users are split rather than all the users to achieve the rate tuple within the capacity region [14], [21]. Analyzing the performance of the uplink RSMA systems with different decoding orders have achieved significant attention recently [22], [23], [24]. In [22], Liu et al. investigated an uplink RSMA system with two users in both general and cognitive radio scenarios wherein specific decoding order and two rate splitting schemes by utilizing fixed power allocation and cognitive power allocation are proposed. The closed-form expressions for both users' OP were derived for different schemes. Moreover, through splitting the signals and allocating the transmit power efficiently at the secondary user, a new RS strategy was proposed for cognitive radio-inspired NOMA systems to enhance the achievable rate of the cognitive user in [23]. The performance of an RSMA system with two users was investigated based on arbitrary decoding order and the closed-form expression of OP was derived in [24].

Compared to NOMA, the RSMA scheme has many advantages: higher spectral efficiency, higher multiplexing gain, more general conditions, suitability for multiple antennas, and lower receiver complexity [11], [13], [14], [25]. On the other hand, despite extremely high data rates in mmWave communication, a much shorter wavelength facilitates equipping more antennas in a limited space, which brings the antenna gain to compensate for the severe path loss. A new hybrid precoding scheme for mmWave systems was proposed to reduce the complexity of the feedback [26]. Their results showed that the RSMA scheme could save the channel training and feedback overhead. However, it is difficult to obtain the closed-form expression for the achievable rate in partially overlapped angle of departure (AoD) scenarios due to the complicated structure of the digital precoder [26].

B. Motivation and Contributions

To the best of our knowledge, it is still an open issue to analyze the performance of the mmWave system with the RSMA scheme, which motivates this work. The main contributions of this paper can be summarized as follows:

1) In this work, we investigate the outage performance of the mmWave RSMA MISO system with a fixed-located user and a randomly located user. Based on the spatial correlation of the paired users and the principle of the RSMA scheme, two beamforming schemes are proposed to improve the reliability of the mmWave RSMA system. Utilizing stochastic geometry theory, the closed-form expressions of the OP with proposed schemes are derived.
2) To obtain more insights, the expressions for the asymptotic OP are derived and the effects of the system parameters are investigated. The results demonstrate that there exists an optimal power allocation coefficient and an optimal number of resolvable paths to minimize the OP of both users. The optimal power allocation coefficients depend on many parameters, such as channel parameters, resolvable paths and path loss exponent, target rates of common streams and private streams, total transmit power of RSMA users, and beamforming scheme.
3) Differing from [10] wherein the beamforming schemes were developed to enhance the secrecy performance of mmWave NOMA networks, beamforming schemes are proposed to improve the reliability of the mmWave RSMA system in this work. Based on the relationship between NOMA and RSMA, the scenarios considered in this work are more generalized.
4) Relative to [20] wherein analytical expressions for average sum-rate were derived by getting analytical ergodic data rate expressions for common and private streams based on stochastic geometry theory, the outage performance of millimeter wave RSMA MISO systems is investigated in this work. The channels in the millimeter wave band are not independent but rather correlated fading for their sparse scattering and multipath, which makes the performance analysis more challenging.

C. Organization

The rest of this paper is organized as follows. Section II describes the system model. Section III proposes two transmission schemes for the mmWave RSMA MISO system. The exact and asymptotic outage performance of mmWave RSMA

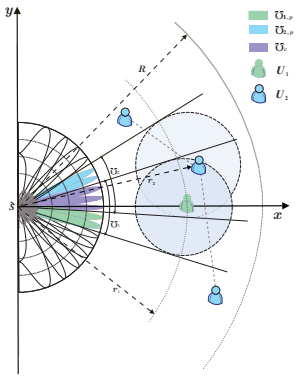

Fig. 1: System model demonstrating a base station (S) and two users (U_1 and U_2).

networks with proposed schemes are analyzed in Sections IV and V, respectively. Section VI presents the numerical and simulation results to demonstrate the analysis and the paper is concluded in Section VII.

II. System Model

As shown in Fig. 1, we consider a downlink mmWave RSMA system, which consists of a base station (S) with N_t antennas and two single-antenna users (U_1 and U_2). Without loss of generality, it is assumed S is located at the origin of a disk with radius R and U_1 is situated at a distance r_1 from the S. It is also assumed that U_2 is randomly distributed on the disk with radius r_2. [1]

Messages W_1 and W_2 are transmitted for U_1 and U_2, respectively. Based on RSMA principle [27], [28], W_i $(i = 1, 2)$ is split into two parts, $\{W_{c,i}, W_{p,i}\}$. Using a codebook shared by both users, $W_{c,1}$ and $W_{c,2}$ are encoded together into a common stream s_c, which is required to be decoded by both users. At the same time, $W_{p,1}$ and $W_{p,2}$ are encoded into the private streams s_1 and s_2, respectively. Then, the transmitted signal from S is given as

$$\mathbf{x} = \mathbf{w}_c\sqrt{P\tau_c}s_c + \mathbf{w}_1\sqrt{P\tau_1}s_1 + \mathbf{w}_2\sqrt{P\tau_2}s_2, \qquad (1)$$

where $\mathbf{w}_c$, $\mathbf{w}_1$, and $\mathbf{w}_2$ are unit vectors that span the beamforming direction, P signifies the transmit power, and τ_c and τ_i denote the power allocation coefficients for s_c and s_i, respectively.

Utilizing the uniform linear array (ULA) model, the channels between S and U_i is expressed as [7]-[10]

$$\mathbf{h}_i = \sqrt{\frac{N_t P_L(r_i)}{L_i}}\mathbf{g}_i\mathbf{U}^H, \qquad (2)$$

where $P_L(r_i) = r_0 r_i^{-\alpha}$, $r_0 = 10^{-\frac{\beta_L}{10}}$, $\beta_L = 32.4 + 20\log_{10}(f_c)$, $f_c = 28$ GHz [29], r_i is the distance between the transmitter and the receiver, α is the path loss exponent, $\mathbf{g}_i = [g_{i,1}, g_{i,2}, \ldots, g_{i,N_t}]$ is the complex gain vector, $\mathbf{U} = [\mathbf{a}(\Psi_1), \mathbf{a}(\Psi_2), \ldots, \mathbf{a}(\Psi_{N_t})]$ is the spatially orthogonal basis, where $\mathbf{a}(\Psi_n) = \frac{1}{\sqrt{N_t}}\left[1, e^{-j\frac{2\pi d}{\lambda}\Psi_n}, e^{-j2\frac{2\pi d}{\lambda}\Psi_n}, \cdots, e^{-j(N_t-1)\frac{2\pi d}{\lambda}\Psi_n}\right]^T$, $\Psi_n = \frac{1}{M}\left(n - 1 - \frac{N_t-1}{2}\right)$ $(n = 1, 2, \ldots, N_t)$ is one-to-one mapping with AoD denoted by $\theta_n = \arcsin(\Psi_n)$, $M = \frac{dN_t}{\lambda}$ is the normalized length of the transmitting antenna and determines angular domain resolvability, d is antenna spacing, λ is wavelength, $L_i = \left\lfloor M\sin(\theta_{i,\max}) + \frac{N_t+1}{2}\right\rfloor - \left\lceil M\sin(\theta_{i,\min}) + \frac{N_t+1}{2}\right\rceil + 1 < N_t$ denotes the number of resolvable paths of U_i, $\theta_{i,\min}$ is the minimum AoD for U_i's all paths, $\theta_{i,\max}$ is the maximum AoD for U_i's all paths, and $g_{i,n} \sim CN(0,1)$ if $\theta_n \in [\theta_{i,\min}, \theta_{i,\max}]$ otherwise $g_{i,n} = 0$ [7].

Based on the spatial correlation of the paired users, the user's paths are divided into common (overlapped) and private (non-overlapped) paths. For tractability of analysis, it is assumed that $L_1 = L_2 = L$ and there are L_c common paths between U_1 and U_2. It must be noted that L_c is a random variable due to the randomness of U_2's location and the probability mass function (PMF) of L_c is given as $\Pr\{L_c = k\} = \omega_k$, where $\omega_k = \frac{2}{\pi}\left(\arcsin\left(\Psi_{\frac{N_t-L}{2}+k+1}\right) - \arcsin\left(\Psi_{\frac{N_t-L}{2}+k}\right)\right)$ for $k = 1, ..., L-1$, $\omega_L = \frac{1}{\pi}\arcsin\left(\Psi_{\frac{N_t+L}{2}+1}\right) - \frac{1}{\pi}\arcsin\left(\Psi_{\frac{N_t+L}{2}}\right)$, and $\omega_0 = 1 - \sum_{j=1}^{L}\omega_j$ [8].

Since U_2 follows uniform distribution in a circle with radius R, the PDF of r_2 is expressed as [10]

$$f_{r_2}(r) = \frac{2r}{R^2}, 0 \le r \le R. \qquad (3)$$

III. Beamforming Schemes

In this section, two beamforming schemes are proposed to provide reliable communication for downlink mmWave RSMA MISO systems.

A. Transmit common messages on the common paths (TCCP)

Based on the spatial correlation of U_1 and U_2, and the principle of the RSMA scheme, we propose a beamforming scheme TCCP wherein s_c is transmitted on the common paths and s_i is transmitted on their own private paths. TCCP can exactly eliminate the inter-user interference of private signals by utilizing the spatial correlation of two users' channels. It is assumed that the perfect channel state information (CSI), including the AoDs and the complex path gains $\mathbf{g}_i$ for two users, is available at S to enable precoding. [2]. The beamform-

[1] Although U_1 is fixed and U_2 is randomly distributed in our work, the results can be easily extended to the downlink mmWave RSMA system with two random users. Similar to [11], [12], [18], [25], the RSMA system with two users is considered in this work. As such, the results in this paper can serve as a benchmark for the performance of such systems. The performance of RSMA systems with multiple users will be part of our future work.

[2] The CSI at the receiver can be obtained via training and subsequently feedback to the S to generate the beamforming vectors [2], [9], [26], [30]. Specifically, the $\mathbf{w}_c^{\mathrm{TCCP}}$ can be generated as per the following steps. Firstly, S sends beam training with receivers. Then, every receiver estimates CSI and subsequently feeds back the index of the analog precoder ($\mathbf{U}_c$) to the S. S trains the effective channels ($\mathbf{h}_i\mathbf{U}_c = \sqrt{\frac{N_t P_L(r_i)}{L}}\mathbf{g}_{i,c}$) with receivers and subsequently gets the quantized channel vector. Finally, S designs its digital precoder ($\frac{\mathbf{g}_{1,c}^H}{\|\mathbf{g}_{1,c}\|}$) based on the quantized CSI. It is assumed that quantization error for quantized channel vector is negligible to guarantee the analytic result.

ing vector for s_c is designed as

$$\mathbf{w}_c^{\mathrm{TCCP}} = \frac{\left(\mathbf{g}_{1,c}\mathbf{U}_c^H\right)^H}{\|\mathbf{g}_{1,c}\mathbf{U}_c^H\|} \in \mathbb{C}^{N_t\times 1}, \tag{4}$$

where $\mathbf{g}_{1,c} = \mathcal{S}(\mathbf{g}_1, \mho_c) \in \mathbb{C}^{1\times L_c}$, $\mathbf{U}_c = \mathcal{S}(\mathbf{U}, \mho_c) \in \mathbb{C}^{N_t\times L_c}$, $\mathcal{S}(\mathbf{B}, D)$ is utilized to generate a new matrix with columns selected from $\mathbf{B}$ based on the selected column index set D, and $\mho_c$ denotes the index set of common resolvable paths between the receivers U_1 and U_2.

Similarly, the beamforming vector for s_i is expressed as

$$\mathbf{w}_i = \frac{\left(\mathbf{g}_{i,p}\mathbf{U}_{i,p}^H\right)^H}{\left\|\mathbf{g}_{i,p}\mathbf{U}_{i,p}^H\right\|} \in \mathbb{C}^{N_t\times 1}, \tag{5}$$

where $\mathbf{g}_{i,p} = \mathcal{S}(\mathbf{g}_i, \mho_{i,p}) \in \mathbb{C}^{1\times L_p}$, $\mathbf{U}_{i,p} = \mathcal{S}(\mathbf{U}, \mho_{i,p}) \in \mathbb{C}^{N_t\times L_p}$, and $\mho_{i,p}$ denotes the index set of the private paths of receiver U_i.

According to the RSMA principle, U_i decodes s_c firstly by treating all the other signals as noise. When $0 < L_c < L$, the instantaneous signal to interference plus noise ratio (SINR) of decoding s_c at U_1 is

$$\begin{aligned}\gamma_{c,1,L_c}^{\mathrm{TCCP}} &= \frac{P\tau_c\|\mathbf{h}_1\mathbf{w}_c\|^2}{P\tau_1\|\mathbf{h}_1\mathbf{w}_1\|^2 + P\tau_2\|\mathbf{h}_1\mathbf{w}_2\|^2 + \sigma_n^2} \\ &\overset{(a)}{=} \frac{P\tau_c\|\mathbf{h}_1\mathbf{w}_c\|^2}{P\tau_1\|\mathbf{h}_1\mathbf{w}_1\|^2 + \sigma_n^2} \\ &\overset{(b)}{=} \frac{\delta_c\|\mathbf{g}_{1,c}\|^2}{\delta_1\|\mathbf{g}_{1,p}\|^2 + 1},\end{aligned} \tag{6}$$

where $\mathbf{h}_1$ is the channel between S and U_1, $\delta_c = \frac{\delta\tau_c}{r_1^\alpha}$, $\delta_1 = \frac{\delta\tau_1}{r_1^\alpha}$, $\rho = \frac{P}{\sigma^2}$, $\delta = \frac{N_t\rho r_0}{L}$, σ_n^2 signifies the noise power at U_1, step (a) is obtained due to $\|\mathbf{h}_1\mathbf{w}_2\|^2 = 0$, and step (b) is obtained based on the definition of $\mathbf{h}_1$ and (4) and (5).

After performing SIC, i.e., the s_c is re-encoded, precoded, and removed from the received signal, the SINR of decoding s_1 at U_1 is obtained as

$$\begin{aligned}\gamma_{p,1,L_c}^{\mathrm{TCCP}} &= \frac{P\tau_1\|\mathbf{h}_1\mathbf{w}_1\|^2}{P\tau_2\|\mathbf{h}_1\mathbf{w}_2\|^2 + \sigma_n^2} \\ &= \delta_1\|\mathbf{g}_{1,p}\|^2.\end{aligned} \tag{7}$$

Remark 1. *Based on (6) and (7), one can find that both $\gamma_{c,1,L_c}^{\mathrm{TCCP}}$ and $\gamma_{p,1,L_c}^{\mathrm{TCCP}}$ would be the bottleneck of RSMA systems. As τ_c increases, $\gamma_{c,1,L_c}^{\mathrm{TCCP}}$ increases and $\gamma_{p,1,L_c}^{\mathrm{TCCP}}$ decreases , thus, there exists an optimal τ_c to minimize the OP of U_1.*

Due to $\|\mathbf{h}_2\mathbf{w}_1\|^2 = 0$, $\gamma_{c,2,L_c}^{\mathrm{TCCP}}$ and $\gamma_{p,2,L_c}^{\mathrm{TCCP}}$ are obtained as

$$\begin{aligned}\gamma_{c,2,L_c}^{\mathrm{TCCP}} &= \frac{P\tau_c\|\mathbf{h}_2\mathbf{w}_c\|^2}{P\tau_2\|\mathbf{h}_2\mathbf{w}_2\|^2 + \sigma_n^2} \\ &= \frac{\delta\tau_c r_2^{-\alpha}\left|\mathbf{g}_2\mathbf{U}^H\mathbf{U}_c\frac{\mathbf{g}_{1,c}^H}{\|\mathbf{g}_{1,c}\|}\right|^2}{\delta\tau_2 r_2^{-\alpha}\|\mathbf{g}_{2,p}\|^2 + 1} \\ &= \frac{\delta\tau_c r_2^{-\alpha}\left|\mathbf{g}_{2,c}\frac{\mathbf{g}_{1,c}^H}{\|\mathbf{g}_{1,c}\|}\right|^2}{\delta\tau_2 r_2^{-\alpha}\|\mathbf{g}_{2,p}\|^2 + 1},\end{aligned} \tag{8}$$

$$\gamma_{p,2,L_c}^{\mathrm{TCCP}} = \delta\tau_2 r_2^{-\alpha}\|\mathbf{g}_{2,p}\|^2, \tag{9}$$

respectively.

To facilitate analysis, we define $v_{i,p}$ $\mu_{c,i} = \|\mathbf{g}_{i,c}\|^2$, $v_{i,p} = \|\mathbf{g}_{i,p}\|^2$, and $\vartheta_i = \|\mathbf{g}_i\|^2$. The PDF and cumulative distribution function (CDF) of $X \in \{\mu_{c,i}, v_{i,p}, \vartheta_i\}$ are expressed as

$$f_X(x) = \frac{e^{-x}x^{\kappa_X - 1}}{(\kappa_X - 1)!}, \tag{10}$$

$$F_X(x) = 1 - e^{-x}\sum_{t=0}^{\kappa_X - 1}\frac{x^t}{t!}, \tag{11}$$

respectively, where $\kappa_{\mu_{c,i}} = L_c$, $\kappa_{v_{i,p}} = L - L_c = L_p$, and $\kappa_{\vartheta_i} = L$. Similarly, we denote $\zeta = \left|\mathbf{g}_2\frac{\mathbf{g}_1{}^H}{\|\mathbf{g}_1\|}\right|^2$ and $\zeta_c = \left|\mathbf{g}_{2,c}\frac{\mathbf{g}_{1,c}^H}{\|\mathbf{g}_{1,c}\|}\right|^2$. The PDF and CDF of $Y \in \{\zeta, \zeta_c\}$ are expressed as $f_Y(y) = e^{-y}$ and $F_Y(y) = 1 - e^{-y}$, respectively [7].

Specifically, RSMA would degenerate as SDMA when $L_c = 0$ and multicast when $L_c = L$ [11], [12]. When $L_c = 0$, there are no overlapped paths between U_1 and U_2, and SDMA scheme is utilized, which means all signals are transmitted in their own private paths with $\tau_c = 0$ and $\gamma_{c,1,0}^{\mathrm{TCCP}} = \gamma_{c,2,0}^{\mathrm{TCCP}} = 0$. The SNR of U_1 and U_2 are expressed as $\gamma_{p,1,0}^{\mathrm{TCCP}} = \delta_1\vartheta_1$ and $\gamma_{p,2,0}^{\mathrm{TCCP}} = \delta\tau_2 r_2^{-\alpha}\vartheta_2$, respectively. When $L_c = L$, there are no private paths and multicasting scheme is utilized, which means all signals are transmitted in the common paths. In this scenario, we have $\tau_1 = \tau_2 = 0$, $\tau_c = 1$, and $\gamma_{p,1,L}^{\mathrm{TCCP}} = \gamma_{p,2,L}^{\mathrm{TCCP}} = 0$. The SINR of U_1 and U_2 are expressed as $\gamma_{c,1,L}^{\mathrm{TCCP}} = \delta r_1^{-\alpha}\vartheta_1$ and $\gamma_{c,2,L}^{\mathrm{TCCP}} = \delta r_2^{-\alpha}\zeta$, respectively.

B. Transmit common messages on all the paths (TCAP)

The TCCP takes natural advantage of common paths to send common messages. However, it does not fully use the benefits of RSMA to transmit messages, i.e., common messages can be removed by SIC and do not interfere with private messages. Thus, transmitting common messages only on common paths while private paths are not utilized to send common messages leads to degraded reception quality at the users. To solve this problem, a new beamforming scheme wherein the common messages are transmitted on the common paths and private paths, termed as TCAP, is proposed in this subsection. Hence, we have

$$\mathbf{w}_c^{\mathrm{TCAP}} = \mathcal{S}(\mathbf{U}, \mho_c + \mho_{1,p} + \mho_{2,p}) \in {}^{N_t\times(2L - L_c)}. \tag{12}$$

It must be noted that the TCAP scheme is a form of analog beamforming since the columns in $\mathbf{w}_c^{\mathrm{TCAP}}$ are all array response vectors and only the signal phase is modified [4], [9]. For the beam of the private signal $\mathbf{w}_i$, it remains the same as TCCP.

Based RSMA principle, the SINR of decoding s_c and s_1 at U_1 are obtained as

$$\gamma_{c,1,L_c}^{\mathrm{TCAP}} = \frac{\delta_c\|\mathbf{g}_1\|^2}{\delta_1\|\mathbf{g}_{1,p}\|^2 + 1}, \tag{13}$$

$$\gamma_{p,1,L_c}^{\mathrm{TCAP}} = \delta_1\|\mathbf{g}_{1,p}\|^2, \tag{14}$$

respectively. Similarly, the SINR of decoding s_c and s_2 at U_2 are obtained as

$$\gamma_{c,2,L_c}^{\mathrm{TCAP}} = \frac{\delta\tau_c r_2^{-\alpha}\|\mathbf{g}_2\|^2}{\delta\tau_2 r_2^{-\alpha}\|\mathbf{g}_{2,p}\|^2+1}, \tag{15}$$

$$\gamma_{p,2,L_c}^{\mathrm{TCAP}} = \delta\tau_2 r_2^{-\alpha}\|\mathbf{g}_{2,p}\|^2, \tag{16}$$

respectively.

Remark 2. *Relative to the TCCP, $\gamma_{c,i,L_c}^{\mathrm{TCAP}}$ is improved due to transmitting in all paths, thus, the $\gamma_{p,i,L_c}^{\mathrm{TCAP}}$ has a higher probability of becoming a bottleneck.*

IV. Outage Probability Analysis

In this work, the outage performance of the RSMA system is investigated because of the following reasons: 1) In some cases, S chooses specific fixed rates within a limited range due to the constraint by the coding and modulation schemes even if the CSI of all the links is available; 2) Even if the global CSI is known, it is useful for S to evaluate the outage performance through OP. In some scenarios, S transmits at a constant rate required in the system regardless of the rate in the channel.

The main steps of the exact OP analysis are listed as follows: 1) According to the total probability theory, the U_i's OP is expressed as the connect probability (CP) of U_i with given $L_c = k$. 2) Derive the CP expression of U_i with $L_c = k$ by utilizing the CDF/PDF of the users' channel gains. 3) Substitute the result of step 2) into step 1) and convert, combine, and simplify the expression for more straightforward calculation to obtain the close-form expression of OP.

According to the law of total probability, the OP of U_i is expressed as

$$\begin{aligned} P_{\mathrm{out},i} &= \sum_{k=0}^{L}\omega_k P_{\mathrm{out},i,k} \\ &= 1-\sum_{k=0}^{L}\omega_k P_{\mathrm{CP},i,k}, \end{aligned} \tag{17}$$

where $P_{\mathrm{CP},i,k} = \Pr\{\gamma_{c,i,k} > \Theta_{c,i}, \gamma_{p,i,k} > \Theta_{p,i}\}$ denotes the CP of U_i with $L_c = k$, $\gamma_{c,i,k}$ and $\gamma_{p,i,k}$ signify the SINR/SNR of the common and private streams, respectively, $\Theta_{c,i} = 2^{R_{c,i}^{\mathrm{th}}}-1$, $\Theta_{p,i} = 2^{R_{p,i}^{\mathrm{th}}}-1$, and $R_{c,i}^{\mathrm{th}}$ and $R_{p,i}^{\mathrm{th}}$ denote the target rates for the common and private streams, respectively. In other words, the link between S and U_i is not in outage when both the common and private rates are larger than desired thresholds, $R_{c,i}^{\mathrm{th}}$ and $R_{p,i}^{\mathrm{th}}$, respectively [16].

A. OP with TCCP

In the following Lemma, we provide the closed-form expression for the CP of U_i for the scenarios with $0 < k < L$ common paths.

Lemma 1. *The CP of U_i with TCCP scheme for $0 < k < L$ is expressed as*

$$P_{\mathrm{CP},i,k}^{\mathrm{TCCP}} = T_{i,k}^{\mathrm{TCCP}} - V_{i,k}^{\mathrm{TCCP}}, \tag{18}$$

where $T_{1,k}^{\mathrm{TCCP}} = e^{-a_4}\sum_{t=0}^{k-1}\frac{a_4^t}{t!} - \sum_{t=0}^{L-k-1}\sum_{n=0}^{t}\chi_1\chi_2$, $\chi_1 = \frac{{a_1}^n(-a_2)^{t-n}e^{a_2}}{n!(t-n)!(k-1)!}$, $\chi_2 = \frac{\Gamma(n+k,a_4(a_1+1))}{(a_1+1)^{n+k}}$, $V_{1,k}^{\mathrm{TCCP}} = e^{-a_4}\sum_{t=0}^{k-1}\frac{a_4^t}{t!}\left(1-e^{-a_3}\sum_{t=0}^{L-k-1}\frac{a_3^t}{t!}\right)$, $a_1 = \frac{\delta_c}{\Theta_{c,1}\delta_1}$, $a_2 = \frac{1}{\delta_1}$, $a_3 = \frac{\Theta_{p,1}}{\delta_1}$, $a_4 = \frac{\Theta_{c,1}(\Theta_{p,1}+1)}{\delta_c}$, $T_{2,k}^{\mathrm{TCCP}} = \phi(b_4,0,R) - \sum_{t=0}^{L-k-1}\sum_{n=0}^{t}\sum_{m=0}^{n}\chi_3\phi(b_1b_4+b_4-b_2,\alpha(t-m),R)$, $b_1 = \frac{\tau_c}{\Theta_{c,2}\tau_2}$, $b_2 = \frac{1}{\delta\tau_2}$, $b_3 = \frac{\Theta_{p,2}}{\delta\tau_2}$, $b_4 = \frac{b_3+b_2}{b_1}$, $V_{2,k}^{\mathrm{TCCP}} = \phi(b_4,0,R) - \sum_{t=0}^{L-k-1}\frac{(b_3)^t\phi(b_3+b_4,\alpha t,R)}{t!}$, $\chi_3 = \frac{{b_4}^{n-m}{b_1}^n(-b_2)^{t-n}}{(t-n)!(n-m)!(b_1+1)^{m+1}}$, $\Theta_{c,i} = 2^{R_{c,i}^{\mathrm{th}}}-1$, $\Theta_{p,i} = 2^{R_{p,i}^{\mathrm{th}}}-1$, $\phi(c,d,R) = \frac{2c^{-\frac{d+2}{\alpha}}}{R^2\alpha}\Upsilon\left(\frac{d+2}{\alpha},cR^\alpha\right)$, $\Upsilon(\cdot,\cdot)$ *and* $\Gamma(\cdot,\cdot)$ *are the lower and upper incomplete Gamma function as defined by [31, (8.350.1)] and [31, (8.350.2)], respectively.*

***Proof*:** See Appendix A.

When $k = 0$, there are no overlapped paths between U_1 and U_2 and SDMA scheme is utilized, which means all signals are transmitted in their own private paths with $\tau_c = 0$ and $\gamma_{c,1,0}^{\mathrm{TCCP}} = \gamma_{c,2,0}^{\mathrm{TCCP}} = 0$. The SNR of U_1 and U_2 are expressed as $\gamma_{p,1,0}^{\mathrm{TCCP}} = \delta_1\vartheta_1$ and $\gamma_{p,2,0}^{\mathrm{TCCP}} = \delta\tau_2 r_2^{-\alpha}\vartheta_2$, respectively. Subsequently, we arrive at the following corollary.

Corollary 1. *Based on (11) and (37), $P_{\mathrm{out},1,0}^{\mathrm{TCCP}}$ is obtained as*

$$P_{\mathrm{out},1,0}^{\mathrm{TCCP}} = 1-\sum_{t=0}^{L-1}\frac{1}{t!}\left(\frac{\Theta_{p,1}}{\delta_1}\right)^t e^{-\frac{\Theta_{p,1}}{\delta_1}}. \tag{19}$$

Similarly, utilizing [31, (8.381.8)], $P_{\mathrm{out},2,0}^{\mathrm{TCCP}}$ is obtained as

$$\begin{aligned} P_{\mathrm{out},2,0}^{\mathrm{TCCP}} &= 1-\sum_{t=0}^{L-1}\frac{1}{t!}\left(\frac{\Theta_{p,2}}{\delta\tau_2}\right)^t\mathbb{E}_{r_2}\left[r_2^{\alpha t}e^{-\frac{\Theta_{p,2}}{\delta\tau_2}r_2^\alpha}\right] \\ &= 1-\sum_{t=0}^{L-1}\frac{2}{\alpha R^2 t!}\left(\frac{\delta\tau_2}{\Theta_{p,2}}\right)^{\frac{2}{\alpha}}\Upsilon\left(t+\frac{2}{\alpha},\frac{\Theta_{p,2}R^\alpha}{\delta\tau_2}\right), \end{aligned} \tag{20}$$

where $\mathbb{E}_A(\cdot)$ is mathematical expectation with respect to A.

When $k = L$, there are no private paths and multicasting scheme is utilized, which means all signals are transmitted in the common paths. In this scenario, we have $\tau_1 = \tau_2 = 0$, $\tau_c = 1$, and $\gamma_{p,1,L}^{\mathrm{TCCP}} = \gamma_{p,2,L}^{\mathrm{TCCP}} = 0$. The SINR of U_1 and U_2 are expressed as $\gamma_{c,1,L}^{\mathrm{TCCP}} = \delta r_1^{-\alpha}\vartheta_1$ and $\gamma_{c,2,L}^{\mathrm{TCCP}} = \delta r_2^{-\alpha}\zeta$, respectively. Subsequently, we arrive at **Corollary 2**.

Corollary 2. *Based on (11) and (37), $P_{\mathrm{out},1,L}^{\mathrm{TCCP}}$ and $P_{\mathrm{out},2,L}^{\mathrm{TCCP}}$ are obtained as*

$$P_{\mathrm{out},1,L}^{\mathrm{TCCP}} = 1-e^{-\frac{\Theta_{c,1}}{\delta r_1^{-\alpha}}}\sum_{t=0}^{L-1}\frac{1}{t!}\left(\frac{\Theta_{c,1}}{\delta r_1^{-\alpha}}\right)^t, \tag{21}$$

$$P_{\mathrm{out},2,L}^{\mathrm{TCCP}} = 1-\frac{2}{\alpha R^2}\left(\frac{\delta}{\Theta_{c,2}}\right)^{\frac{2}{\alpha}}\Upsilon\left(\frac{2}{\alpha},\frac{\Theta_{c,2}}{\delta}R^\alpha\right), \tag{22}$$

respectively.

By substituting (18)-(22) into (17), we obtain the following theorem.

$$P_{\mathrm{CP},1,k}^{\mathrm{TCAP}}=\begin{cases}\bar{F}_{\mu_{c,1}}\left(a_7\right)\bar{F}_{v_1}\left(a_3\right)-\sum\limits_{t=0}^{L-k-1}\sum\limits_{n=0}^{t}\chi_4\chi_5, & a_1<1\\ \bar{F}_{v_1}\left(a_3\right)\bar{F}_{\mu_{c,1}}\left(a_7\right)+\sum\limits_{t=0}^{L-k-1}\sum\limits_{n=0}^{t}\sum\limits_{m=0}^{k-1}\chi_6\chi_7, & a_1>1,a_7>0\\ \bar{F}_{v_1}\left(a_3\right), & a_1>1,a_7\leq 0\\ \bar{F}_{\mu_{c,1}}\left(a_2\right)\bar{F}_{v_1}\left(a_3\right), & a_1=1\end{cases} \tag{25}$$

Theorem 1. *The OP of U_1 with TCCP scheme is expressed as*

$$\begin{aligned}P_{\mathrm{out},1}^{\mathrm{TCCP}}=&1-\sum_{t=0}^{L-1}\frac{1}{t!}\left(\omega_0\left(\frac{\Theta_{p,1}r_1^{\alpha}}{\delta\tau_1}\right)^t e^{-\frac{\Theta_{p,1}r_1^{\alpha}}{\delta\tau_1}}\right.\\&\left.+\omega_L\left(\frac{\Theta_{c,1}r_1^{\alpha}}{\delta}\right)^t e^{-\frac{\Theta_{c,1}r_1^{\alpha}}{\delta}}\right)\\&-\sum_{k=1}^{L-1}\omega_k\left(T_{1,k}^{\mathrm{TCCP}}-V_{1,k}^{\mathrm{TCCP}}\right).\end{aligned} \tag{23}$$

The OP of U_2 with TCCP scheme is expressed as

$$\begin{aligned}P_{\mathrm{out},2}^{\mathrm{TCCP}}=&1-\frac{2\omega_0}{\alpha}\left(\frac{R^{\alpha}\Theta_{p,2}}{\delta\tau_2}\right)^{-\frac{2}{\alpha}}\sum_{t=0}^{L-1}\frac{1}{t!}\Upsilon\left(t+\frac{2}{\alpha},\frac{R^{\alpha}\Theta_{p,2}}{\delta\tau_2}\right)\\&-\frac{2\omega_L}{\alpha}\left(\frac{R^{\alpha}\Theta_{c,2}}{\delta}\right)^{-\frac{2}{\alpha}}\Upsilon\left(\frac{2}{\alpha},\frac{R^{\alpha}\Theta_{c,2}}{\delta}\right)\\&-\sum_{k=1}^{L-1}\omega_k\left(T_{2,k}^{\mathrm{TCCP}}-V_{2,k}^{\mathrm{TCCP}}\right).\end{aligned} \tag{24}$$

B. OP with TCAP

In this subsection, we investigate the outage performance of the mmWave RSMA MISO system with TCAP scheme.

In the following Lemmas, we provide the closed-form expression for the CP of U_i with $0<k<L$.

Lemma 2. *When $0<k<L$, $P_{\mathrm{CP},1,k}^{\mathrm{TCAP}}$ is expressed as (25), shown at the top of this page, where $\chi_4=\frac{{a_5}^n(-a_6)^{t-n}e^{a_6}}{(t-n)!n!(k-1)!}$, $a_5=\frac{a_1}{1-a_1}$, $a_6=\frac{a_2}{1-a_1}$, $a_7=\frac{(1-a_1)a_3+a_2}{a_1}$, $\chi_5=\frac{\Gamma(n+k,(a_5+1)a_7)}{(a_5+1)^{n+k}}$, $\chi_6=\frac{(-1)^{t-n}a_5^n a_6^{t+k-n-m-1}}{(a_5+1)^{t+k}(k-m-1)!(t-n)!n!m!}$, $\chi_7=\Upsilon\left(n+m+1,\left(a_5+1\right)a_7-a_6\right)-\Upsilon\left(n+m+1,-a_6\right)$, and $\bar{F}_X\left(\cdot\right)=1-F_X\left(\cdot\right)$ denotes the complementary CDF (CCDF) of X.*

***Proof*:** See Appendix B.

Lemma 3. *When $0<k<L$, $P_{\mathrm{CP},2,k}^{\mathrm{TCAP}}$ is expressed as (26), shown at the top of next page, where $\chi_8=\frac{b_5^m(-b_6)^{t-m}}{(t-m)!m!(k-1)!}$, $\chi_9=\sum\limits_{z=0}^{k+m-1}\frac{b_7^z(k+m-1)!\phi(b_5b_7+b_7-b_6,\alpha(t-m+z),R)}{z!(b_5+1)^{k+m-z}}$, $\chi_{11}=\sum\limits_{z=0}^{n+m}\left(\chi_{12}-\chi_{13}\right)$, $\chi_{10}=\frac{b_5^m(-b_6)^{t-m}b_6^{k-n-1}}{(k-n-1)!(t-m)!m!n!(b_5+1)^{t+k}}$, $\chi_{12}=\frac{(n+m)!(-b_6)^z\phi(-b_6,\alpha(t-n+k-m-1+z),R)}{z!}$, $\chi_{13}=\frac{(n+m)!(b_5b_7+b_7-b_6)^z}{z!}$ $\phi\left(b_5b_7+b_7-b_6,\alpha\left(t-n+k-m-1+z\right),R\right)$, $b_5=\frac{b_1}{1-b_1}$, $b_6=\frac{b_2}{1-b_1}$, and $b_7=\frac{(1-b_1)b_3+b_2}{b_1}$.*

***Proof*:** See Appendix C.

When $k=0$, due to $\gamma_{c,1,0}^{\mathrm{TCAP}}=\gamma_{c,2,0}^{\mathrm{TCAP}}=0$, $\gamma_{p,1,0}^{\mathrm{TCAP}}=\gamma_{p,1,0}^{\mathrm{TCCP}}$ and $\gamma_{p,2,0}^{\mathrm{TCAP}}=\gamma_{p,2,0}^{\mathrm{TCCP}}$, we derive $P_{\mathrm{out},1,0}^{\mathrm{TCAP}}=P_{\mathrm{out},1,0}^{\mathrm{TCCP}}$ and $P_{\mathrm{out},2,0}^{\mathrm{TCAP}}=P_{\mathrm{out},2,0}^{\mathrm{TCCP}}$.

When $k=L$, because of $\gamma_{p,1,L}^{\mathrm{TCAP}}=\gamma_{p,2,L}^{\mathrm{TCAP}}=0$, $\gamma_{c,1,L}^{\mathrm{TCAP}}=\gamma_{c,1,L}^{\mathrm{TCCP}}$ and $\gamma_{c,2,L}^{\mathrm{TCAP}}=\delta r_2^{-\alpha}\vartheta_2$. Thus, $P_{\mathrm{out},1,L}^{\mathrm{TCAP}}=P_{\mathrm{out},1,L}^{\mathrm{TCCP}}$. Based on (11), $P_{\mathrm{out},2,L}^{\mathrm{TCAP}}$ is obtained as

$$P_{\mathrm{out},2,L}^{\mathrm{TCAP}}=1-\sum_{t=0}^{L-1}\frac{1}{t!}\left(\frac{\Theta_{c,2}}{\delta}\right)^t\phi\left(\frac{\Theta_{c,2}}{\delta},\alpha t,R\right). \tag{27}$$

By substituting (19), (20), (21), (25), (26), and (27) into (17), we derive the following theorem.

Theorem 2. *The OP of U_1 with TCAP scheme is expressed as*

$$\begin{aligned}P_{\mathrm{out},1}^{\mathrm{TCAP}}=&1-\sum_{t=0}^{L-1}\frac{1}{t!}\left(\omega_0\left(\frac{\Theta_{p,1}r_1^{\alpha}}{\delta\tau_1}\right)^t e^{-\frac{\Theta_{p,1}r_1^{\alpha}}{\delta\tau_1}}\right.\\&\left.+\omega_L\left(\frac{\Theta_{c,1}r_1^{\alpha}}{\delta}\right)^t e^{-\frac{\Theta_{c,1}r_1^{\alpha}}{\delta}}\right)-\sum_{k=1}^{L-1}\omega_k P_{\mathrm{CP},1,k}^{\mathrm{TCAP}}.\end{aligned} \tag{28}$$

The OP of U_2 with TCAP scheme is expressed as

$$\begin{aligned}P_{\mathrm{out},2}^{\mathrm{TCAP}}=&1-\frac{2\omega_0}{\alpha}\left(\frac{R^{\alpha}\Theta_{p,2}}{\delta\tau_2}\right)^{-\frac{2}{\alpha}}\sum_{t=0}^{L-1}\frac{1}{t!}\Upsilon\left(t+\frac{2}{\alpha},\frac{R^{\alpha}\Theta_{p,2}}{\delta\tau_2}\right)\\&-\frac{2\omega_L}{\alpha}\left(\frac{R^{\alpha}\Theta_{c,2}}{\delta}\right)^{-\frac{2}{\alpha}}\sum_{t=0}^{L-1}\frac{1}{t!}\Upsilon\left(t+\frac{2}{\alpha},\frac{R^{\alpha}\Theta_{c,2}}{\delta}\right)\\&-\sum_{k=1}^{L-1}\omega_k P_{\mathrm{CP},2,k}^{\mathrm{TCAP}}.\end{aligned} \tag{29}$$

The analytical expressions provided in ***Theorem 1*** and ***Theorem 2*** are complicated since many factors affect the outage performance, specifically, power allocation coefficient, the target data rate of s_c and s_i, resolvable paths L, and distances r_1 and R. To obtain more insights, we derive the analytical expressions of the asymptotic OP in the high transmit power regime in the following section.

V. Asymptotic Outage Probability Analysis

This section investigates the asymptotic OP of the RSMA system with two beamforming schemes. The main steps of the asymptotic OP analysis procedure are listed as follows: 1) Based on the results of the exact OP, the asymptotic OP is expressed as the asymptotic OP of U_i with $L_c=k$. 2) Derive the expression for the asymptotic OP of U_i with $L_c=k$ based on the results at $\rho\to\infty$. 3) Analyze the influence of each

$$P_{\mathrm{CP},2,k}^{\mathrm{TCAP}}=\begin{cases}\sum\limits_{t=0}^{L-k-1}\left(\sum\limits_{n=0}^{k-1}\frac{b_7^n b_3^t\phi(b_3+b_7,\alpha(t+n),R)}{n!t!}-\sum\limits_{m=0}^{t}\chi_8\chi_9\right), & b_1<1\\ \sum\limits_{t=0}^{L-k-1}\sum\limits_{n=0}^{k-1}\left(\frac{b_3^t b_7^n\phi(b_3+b_7,\alpha(t+n),R)}{t!n!}+\sum\limits_{m=0}^{t}\chi_{10}\chi_{11}\right), & b_1>1,b_7>0\\ \sum\limits_{t=0}^{L-k-1}\frac{b_3^t\phi(b_3,\alpha t,R)}{t!}, & b_1>1,b_7\leq 0\\ \sum\limits_{t=0}^{L-k-1}\sum\limits_{n=0}^{k-1}\frac{b_2^n b_3^t\phi(b_2+b_3,\alpha(t+n),R)}{t!n!}, & b_1=1\end{cases} \tag{26}$$

component at $\rho\to\infty$ and keep the main term that has the most dominant impact on OP. 4) Substitute the result of step 3) into step 1), combine, and simplify the expression for the more straightforward calculation to obtain the expression of asymptotic OP.

When $\rho\to\infty$, the asymptotic OP is expressed as

$$P_{\mathrm{out},i}^{\infty}=\sum_{k=0}^{L}\omega_k P_{\mathrm{out},i,k}^{\infty}, \tag{30}$$

where $P_{\mathrm{out},i,k}^{\infty}$ denotes the asymptotic OP of U_i with $L_c=k$.

A. OP with TCCP

Theorem 3. *When $\rho\to\infty$, the asymptotic OP of U_1 is expressed as*

$$P_{\mathrm{out},1}^{\mathrm{TCCP},\infty}=\sum_{k=1}^{L-1}\sum_{t=0}^{L-k-1}\frac{\omega_k a_1^t\,(t+k-1)!}{(k-1)!t!(a_1+1)^{t+k}}. \tag{31}$$

When $\rho\to\infty$, the asymptotic OP of U_2 is expressed as

$$P_{\mathrm{out},2}^{\mathrm{TCCP},\infty}=\sum_{k=1}^{L-1}\sum_{t=0}^{L-k-1}\frac{\omega_k {b_1}^t}{(b_1+1)^{t+1}}. \tag{32}$$

***Proof*:** See Appendix D.

Remark 3. *Based on the results presented in theorem 3, one can realize there is an OP floor, which depends on τ_c or N_t and is independent of r_1 (R).*

Thus, based on $G_d=-\lim\limits_{\rho\to\infty}\frac{\log P_{out}^{\infty}(\rho)}{\log\rho}$, the diversity orders of U_1 and U_2 with TCCP scheme are obtained as $G_1^{\mathrm{TCCP}}=G_2^{\mathrm{TCCP}}=0$.

B. OP with TCAP.

Theorem 4. *When $\rho\to\infty$, the asymptotic OP for U_1 is expressed as*

$$P_{\mathrm{out},1}^{\mathrm{TCAP},\infty}=\begin{cases}\sum\limits_{k=1}^{L-1}\sum\limits_{t=0}^{L-k-1}\frac{\omega_k a_5^t(t+k-1)!}{t!(k-1)!(a_5+1)^{t+k}}, & a_1<1,\\ \omega_{L-1}a_3, & a_1>1,\\ \omega_1 a_2+\omega_{L-1}a_3, & a_1=1.\end{cases} \tag{33}$$

When $\rho\to\infty$, the asymptotic OP for U_2 is expressed as

$$P_{\mathrm{out},2}^{\mathrm{TCAP},\infty}=\begin{cases}\sum\limits_{k=1}^{L-1}\sum\limits_{t=0}^{L-k-1}\frac{\omega_k b_5^t(t+k-1)!}{t!(k-1)!(b_5+1)^{t+k}}, & b_1<1,\\ \frac{2\omega_{L-1}b_3R^{\alpha}}{\alpha+2}, & b_1>1,\\ \frac{2\left(\omega_1 b_2+\omega_{L-1}b_3\right)R^{\alpha}}{\alpha+2}, & b_1=1.\end{cases} \tag{34}$$

***Proof*:** See Appendix E.

Remark 4. *Based on the results presented in theorem 4, one can easily deduce that there is an OP floor when $\tau_c<\Theta_{c,i}\tau_i$. This is because $\gamma_{c,1,k}^{\mathrm{TCAP}}$ is the bottleneck and tends to a constant in large-P region. In other words, OP floor can be avoided effectively by adjusting the power allocation coefficient τ_c in TCAP.*

Thus, the diversity orders of U_1 and U_2 with TCAP scheme are obtained as

$$G_1^{\mathrm{TCAP}}=\begin{cases}0, & a_1<1,\\ 1, & a_1\geq 1,\end{cases} \tag{35}$$

and

$$G_2^{\mathrm{TCAP}}=\begin{cases}0, & b_1<1,\\ 1, & b_1\geq 1,\end{cases} \tag{36}$$

respectively.

VI. Numerical Results

This section presents simulation and numerical results to verify the outage performance of mmWave RSMA systems with the proposed beamforming schemes. The noise power is set at $\sigma^2=-71$ dB [9], [32], [33] and the path-loss model is set as $\alpha=2.1$ [29]. It is assumed that $R_{c,1}^{\mathrm{th}}=R_{c,2}^{\mathrm{th}}=R_c^{\mathrm{th}}$, $R_{p,1}^{\mathrm{th}}=R_{p,2}^{\mathrm{th}}=R_p^{\mathrm{th}}$, and $\tau_1=\tau_2=\tau$. In all the figures, 'Sim' and 'Ana' denote the simulation and numerical results, respectively.

Fig. 2 demonstrates the impact of P for varying r_1 (R) and N_t on OP with TCCP and TCAP schemes. It can be observed that the OP of U_i is improved with increasing P. Unlike the OP with TCAP, the OP with TCCP tends to be a constant in the high-P region. According to the RSMA technology, the common part is decoded first then re-encoded and deleted from the received signals. Finally, the private part is decoded. The common part in the TCCP scheme is sent on overlapped paths while the common part in the TCAP scheme is sent on all the paths of both users. Thus, the OP of the common part in TCCP is higher than that in TCAP. The bottleneck in TCCP is due to decoding the common part while in TCAP it is decoding the private part. Based on the SINR (SNR) expressions for the common and private parts, we can observe that the SINR of the common part converges to a constant as P increases while the SNR of the private part continues to increase with increasing P. Figs. 2(a) and 2(b) present the impact of r_1 (R) on OP with TCCP and TCAP schemes, respectively. We observe that the OP of both users

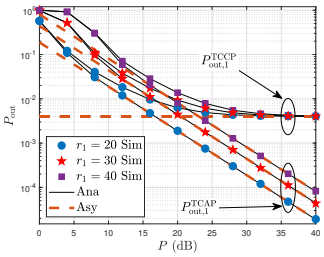

(a) OP for varying r_1 with $N_t = 50$.

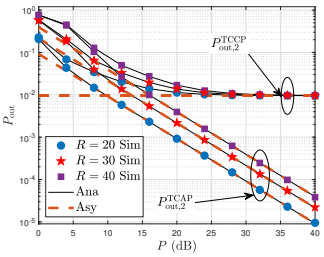

(b) OP for varying R with $N_t = 50$.

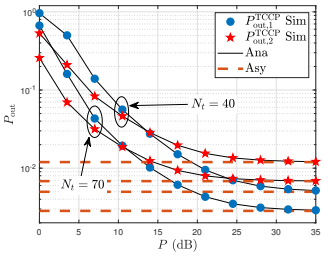

(c) OP with TCCP for varying N_t with $r_1 = R = 25$.

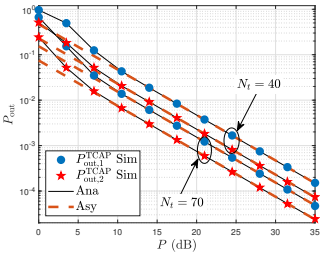

(d) OP with TCAP for varying N_t with $r_1 = R = 25$.

Fig. 2: OP versus the P with $\tau_c = 0.7$, $\tau = 0.15$, $L = 5$, and $R_{\text{c}}^{\text{th}} = R_{\text{p}}^{\text{th}} = 0.25$.

with TCCP and TCAP schemes is deteriorating as r_1 (R) increases since the path loss becomes stronger. In the large-P region, the asymptotic OP with TCCP is independent of r_1 (R) and the asymptotic OP with TCAP depends on r_1 (R) for the same reason as the effect of P on the exact OP. Figs. 2(c) and 2(d) present the impact of N_t on OP with TCCP and TCAP schemes, respectively. The results demonstrate that the OP for both users with TCCP and TCAP schemes is improving as N_t increases and the asymptotic OP in the larger-P region depends on N_t as the quality of the received signal improves. Fig. 2(c) demonstrates that OP of U_2 with TCCP outperforms that of U_1 with TCCP in the low-P region and underperforms that of U_1 with TCCP in the large-P region. This is because power (path loss) is the dominant factor in the low-P region. In the large-P region, the effect from beamforming becomes the dominant factor while the beamforming in TCCP is designed for U_1. Based on Figs. 2(a), 2(b), and 2(d), OP of U_2 with TCAP always outperform that of U_1 with TCAP because the effect of beamforming on both users is the same but the path loss of U_1 is stronger than that of U_2.

Fig. 3 demonstrates the OP vs. P for varying τ_c with TCCP and TCAP schemes, respectively. One can observe that there is a floor for the OP with TCCP while there is a floor for the OP with TCAP only when τ_c is lower, which is testified in *Remark 3* and *Remark 4*. Moreover, based on Figs. 2(a), 2(b), 2(d), and 3(b), it can be observed that the diversity order of OP with TCAP is 1, which is given in *Remark 4*.

Fig. 4 presents the impact of L with varying r_1 (R) and N_t on OP under TCCP and TCAP schemes. It can be observed that the OP initially decreases and then increases as L increases, indicating an optimal L to minimize the OP of the users. It must be noted that the probability that there are common paths between two users with $L = 1$ is the least

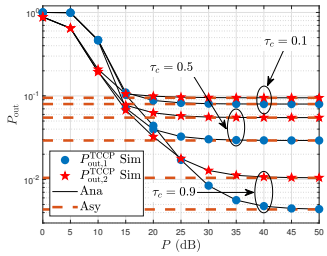

(a) OP with TCCP for varying τ_c.

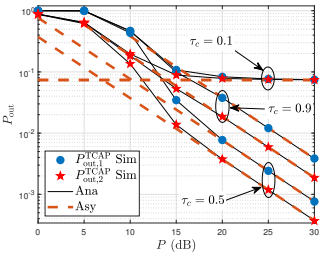

(b) OP with TCAP for varying τ_c.

Fig. 3: OP versus varying P with $N_t = 50$, $L = 5$, $R = r_1 = 25$, and $R_{\text{c}}^{\text{th}} = R_{\text{p}}^{\text{th}} = 0.85$.

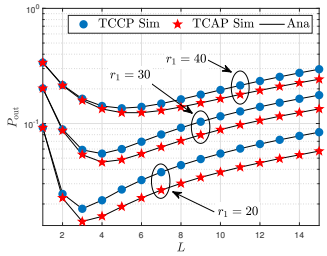

(a) $P_{\text{out},1}$ for varying r_1 with $N_t = 50$.

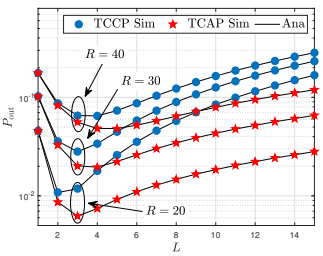

(b) $P_{\text{out},2}$ for varying R with $N_t = 50$.

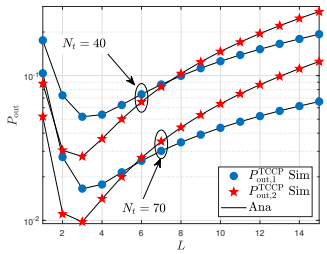

(c) OP with TCCP for varying N_t with $r_1 = R = 25$.

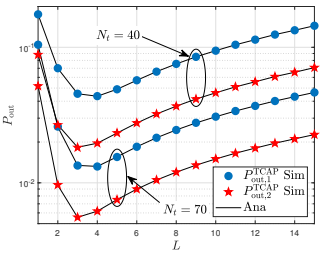

(d) OP with TCAP for varying N_t with $r_1 = R = 25$.

Fig. 4: OP versus varying L with $P = 10$ dB, $\tau_c = 0.7$, $\tau = 0.15$, and $R_{\text{c}}^{\text{th}} = R_{\text{p}}^{\text{th}} = 0.25$.

and the SDMA scheme is utilized with a larger probability. As L increases, the probability that there are common paths increases thereby the number of common paths between two users increases and hence the probability that the RSMA scheme is utilized increases. Thus, the outage performance is improved. In such scenarios with TCCP wherein the common part is the bottleneck of the RSMA system, the larger the L, the stronger the interference from the private part on the common part, thereby the OP is deteriorated. In scenarios with TCAP wherein the private part is the bottleneck of the RSMA system, the larger the L, the lower the power is allocated for each path. Thus, the OP is also worsened. Figs. 4(a) demonstrates that the effect of r_1 (R) on $P_{\text{out},1}$ and Fig. 4(b) demonstrates that the effect of R on $P_{\text{out},2}$. One can observe that larger the r_1, the worse outage performance based on the same reason as experienced in Figs. 2(a) and 2(b). Fig. 4(c) demonstrates the effect of N_t on OP with TCCP and Fig. 4(d) demonstrates the impact of N_t on OP with TCAP. From Figs. 4(b) and 4(c), we can observe that OP of U_2 with TCCP deteriorates faster than

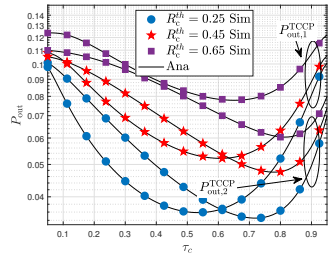

(a) OP with TCCP for varying R_c^{th} with $R_p^{th} = 0.25$.

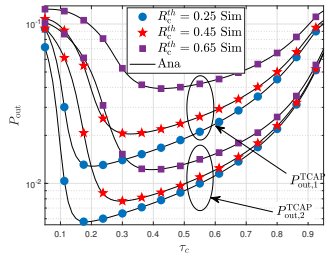

(b) OP with TCAP for varying R_c^{th} with $R_p^{th} = 0.25$.

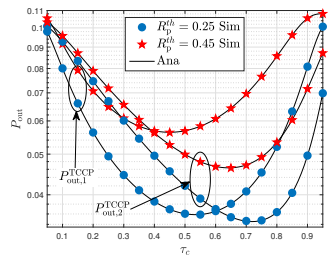

(c) OP with TCCP for varying R_p^{th} with $R_c^{th} = 0.25$.

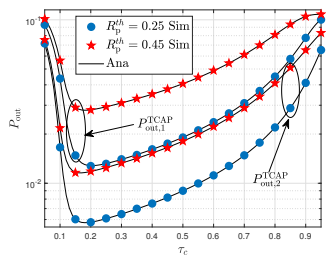

(d) OP with TCAP for varying R_p^{th} with $R_c^{th} = 0.25$.

Fig. 5: OP versus the τ_c with $N_t = 50$, $P = 10$ dB, $L = 5$, and $r_1 = R = 25$.

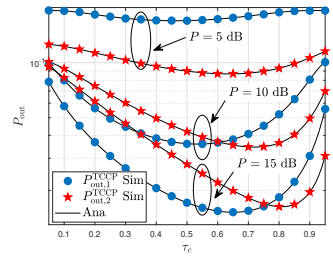

(a) OP with TCCP for varying P.

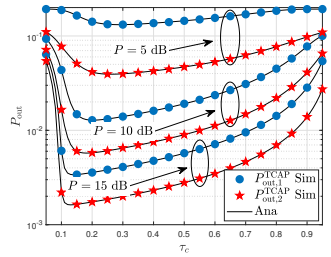

(b) OP with TCAP for varying P.

Fig. 6: OP versus the τ_c with $N_t = 50$, $L = 5$, $R_1 = r_1 = 25$, and $R_c^{th} = R_p^{th} = 0.25$.

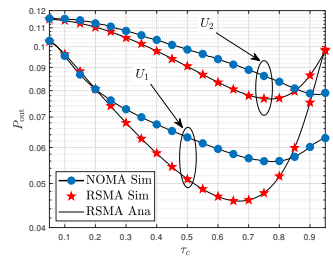

(a) OP with TCCP for varying τ_c.

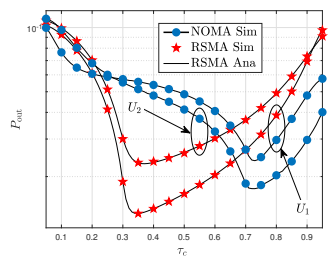

(b) OP with TCAP for varying τ_c.

Fig. 7: OP versus varying τ_c with $N_t = 50$, $L = 5$, $P = 15$ dB, $r_1 = 20$, $R = 30$, and $R_c^{th} = R_p^{th} = 0.85$.

with TCAP or that of U_1 with TCCP since the beamforming can not maximize SINR of U_2 with TCCP.

Fig. 5 demonstrates the OP vs τ_c for varying R_p^{th} and R_c^{th}. One can observe that OP decreases initially and then increases as τ_c increases. The reason is that the power of the common part increases with increasing τ_c thereby the probability of successful decoding increases, and hence the whole OP decreases. However, the power allocated to the private part decreases, and hence the OP of the private part increases, which leads to the deterioration of the whole OP. Furthermore, there is an optimal τ_c to minimize the OP and the optimal τ_c depends on R_p^{th} and R_c^{th}. The optimal τ_c for TCCP is higher than that for TCAP, which indicates that lesser power must be allocated to the common part in TCAP since the common part is transmitted on all paths. More power must be allocated to the common part in TCCP since it is transmitted only on overlapped paths. Figs. 5(a) and 5(c) demonstrate that $P_{out,1}^{TCCP}$ outperforms $P_{out,2}^{TCCP}$ in lower-τ_c region and underperforms $P_{out,2}^{TCCP}$ in larger-τ_c region. This is because the common part is the bottleneck and beamforming for the common part maximizes the SINR of decoding s_c at U_1 in the lower-τ_c region. The private part is the bottleneck in the large-τ_c region and the beamforming for the private part has the same effect on both users. Figs. 5(b) and 5(d) demonstrate that $P_{out,2}^{TCAP}$ outperforms $P_{out,1}^{TCAP}$ since the effects of beamforming are the same for both users and the path loss at U_1 is stronger than that at U_2.

Fig. 6 demonstrates the simulation results of OP vs. τ_c for varying P. We observe that the optimal τ_c depends on P. Fig. 6(a) demonstrates that $P_{out,2}^{TCCP}$ outperforms $P_{out,1}^{TCCP}$ in low-P region with the same reason as in Figs. 2(a) and 2(b). As P increases, $P_{out,1}^{TCCP}$ outperforms $P_{out,2}^{TCCP}$ in lower-τ_c region and underperforms $P_{out,2}^{TCCP}$ in larger-τ_c region, which is same as exhibited in Figs. 5(a) and 5(c). Fig. 6(b) demonstrates that $P_{out,2}^{TCAP}$ outperforms $P_{out,1}^{TCAP}$, which is same as exhibited in Figs. 5(b) and 5(d).

Fig. 7 compares the OP of both users with RSMA and NOMA schemes, respectively. Based on [12], the signals of the near user of the NOMA systems are transmitted on their private paths. The signals for the far user are transmitted on the overlapped paths in 7(a) and on all paths in Fig. 7(b), respectively. It can be observed that the OP with RSMA outperforms that with NOMA in the lower-τ_c region. This is because, in the lower-τ_c region, decoding the signals of the far user behaves as the NOMA system's bottleneck. When more power is allocated to the far user's signals, the NOMA systems' performance will be improved. For the RSMA system, decoding the common streams is the system's bottleneck in the lower-τ_c region. When the power allocated to the signals of the far user in NOMA is equal to that allocated to the common streams in RSMA, the power allocated to the signals of the near user is definitely greater than that allocated to each private stream in RSMA. Thus, the SINR of decoding the common stream in RSMA is greater than that of decoding the signals of the far user at the near users in NOMA.

Similar to [17], to compare the differences between the proposed TCCP and TCAP schemes, we provide some simulation results in Fig. 8 to illustrate the normalized beampatterns of $\mathbf{w}_c^{TCCP}, \mathbf{w}_c^{TCAP}, \mathbf{w}_1$, and $\mathbf{w}_2$. One can observe that the maximal gain direction of common streams points to common paths and all the paths of U_1 and U_2, respectively, while nulls are generated at the other paths with -300 dB. The reason

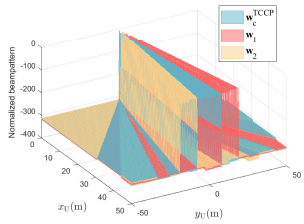

(a) 3D Beampattern of TCCP beamforming scheme.

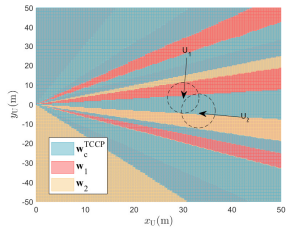

(b) Beampattern of TCCP beamforming scheme from vertical vision (top aerial view).

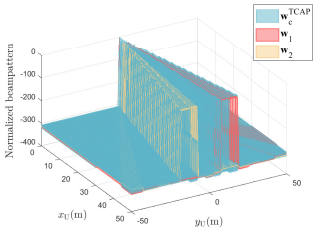

(c) 3D Beampattern of TCAP beamforming scheme.

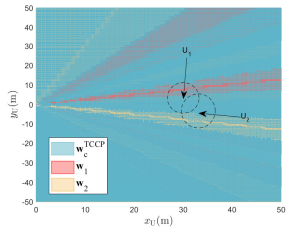

(d) Beampattern of TCAP beamforming scheme from vertical vision (top aerial view).

Fig. 8: Beampattern of TCCP and TCAP beamforming schemes with $N_t = 20$, $L = 5$, $L_c = 3$, $r_1 = 30$, and $R = 40$.

is that $\mathbf{w}_c^{\mathrm{TCCP}}$ and $\mathbf{w}_c^{\mathrm{TCAP}}$ are mapped with the common streams, which are intended for U_1 and U_2 on common paths and all the paths, respectively. The maximal gain direction of private streams points to their private paths, respectively, which demonstrates that the proposed RSMA-based beamforming scheme can eliminate the inter-user interference.

VII. Conclusion

In this work, the outage performance of mmWave RSMA MISO systems has been investigated. Considering the multipath and limited scattering propagation characteristics of mmWave channels and based on the RSMA principle, we proposed two beamforming transmission schemes (i.e., TCCP and TCAP) to enhance reliable performance. The closed-form and asymptotic expressions of OP for users with proposed schemes were derived using stochastic geometry. The results demonstrated that the TCAP scheme could effectively enhance reliability performance while the TCCP scheme is easier to implement while being robust. Moreover, optimal power allocation coefficient and spatially resolvable paths exist to minimize the OP highlighting the importance of the power allocation scheme and users' AoD range. Based on instantaneous CSI or CSI statistics, some potential solutions, such as convex optimization and deep learning, can be utilized to obtain the optimal power allocation coefficients in future work.

Appendix A
Proof of Lemma 1

Based on (6) and (7), the CP of U_1 with $0 < k < L$, $P_{\mathrm{CP},1,k}^{\mathrm{TCCP}}$, is expressed as (37), shown at the top of next page, where $\Theta_{c,1} = 2^{R_{c,1}^{\mathrm{th}}} - 1$, $\Theta_{p,1} = 2^{R_{p,1}^{\mathrm{th}}} - 1$, $a_1 = \frac{\delta_c}{\Theta_{c,1}\delta_1} = \frac{\tau_c}{\Theta_{c,1}\tau_1}$, $a_2 = \frac{1}{\delta_1}$, $a_3 = \frac{\Theta_{p,1}}{\delta_1}$, and $a_4 = \frac{a_3+a_2}{a_1} = \frac{\Theta_{c,1}(\Theta_{p,1}+1)}{\delta_c}$. Based on (10) and (11), and utilizing [31, (1.111)] and [31, (3.351.2)], $T_{1,k}^{\mathrm{TCCP}}$ is obtained as

$$\begin{aligned} T_{1,k}^{\mathrm{TCCP}} &= e^{-a_4}\sum_{t=0}^{k-1}\frac{a_4^t}{t!} - \sum_{t=0}^{L-k-1}\sum_{n=0}^{t}\chi_1 \\ &\quad\times\int_{a_4}^{\infty} e^{-(a_1+1)y}y^{n+k-1}dy \\ &= e^{-a_4}\sum_{t=0}^{k-1}\frac{a_4^t}{t!} - \sum_{t=0}^{L-k-1}\sum_{n=0}^{t}\chi_1\chi_2, \end{aligned} \tag{38}$$

where $\chi_1 = \frac{{a_1}^n(-a_2)^{t-n}e^{a_2}}{n!(t-n)!(k-1)!}$, $\chi_2 = \frac{\Gamma(n+k,a_4(a_1+1))}{(a_1+1)^{n+k}}$, and $\Gamma(\cdot,\cdot)$ is the upper incomplete Gamma function defined by [31, (8.350.2)]. Similarly, $V_{1,k}^{\mathrm{TCCP}}$ is obtained as

$$V_{1,k}^{\mathrm{TCCP}} = F_{v_1}(a_3)\,\bar{F}_{\mu_c}(a_4), \tag{39}$$

where $\bar{F}_X(\cdot) = 1 - F_X(\cdot)$ denotes the complementary CDF (CCDF) of X.

Similar to (37), the CP of U_2 with $0 < k < L$, $P_{\mathrm{CP},2,k}^{\mathrm{TCCP}}$, is obtained as

$$\begin{aligned} P_{\mathrm{CP},2,k}^{\mathrm{TCCP}} &= \Pr\{v_2 < b_1\zeta_c - b_2 r_2^{\alpha}, v_2 > b_3 r_2^{\alpha}\} \\ &= \Pr\{b_3 r_2^{\alpha} < v_2 < b_1\zeta_c - b_2 r_2^{\alpha}, \zeta_c > b_4 r_2^{\alpha}\} \\ &= \underbrace{\mathbb{E}_{r_2}\left[\int_{b_4 r_2^{\alpha}}^{\infty} F_{v_2}(b_1 y - b_2 r_2^{\alpha}) f_{\zeta_c}(y)\,dy\right]}_{\triangleq T_{2,k}^{\mathrm{TCCP}}} \\ &\quad - \underbrace{\mathbb{E}_{r_2}\left[F_{v_2}(b_3 r_2^{\alpha})\int_{b_4 r_2^{\alpha}}^{\infty} f_{\zeta_c}(y)\,dy\right]}_{\triangleq V_{2,k}^{\mathrm{TCCP}}}, \end{aligned} \tag{40}$$

where $\Theta_{c,2} = 2^{R_{c,2}^{\mathrm{th}}} - 1$, $\Theta_{\mathrm{p},2} = 2^{R_{\mathrm{p},2}^{\mathrm{th}}} - 1$, $b_1 = \frac{\tau_c}{\Theta_{c,2}\tau_2}$, $b_2 = \frac{1}{\delta\tau_2}$, $b_3 = \frac{\Theta_{\mathrm{p},2}}{\delta\tau_2}$, $b_4 = \frac{b_3+b_2}{b_1} = \frac{\Theta_{c,2}(\Theta_{\mathrm{p},2}+1)}{\delta\tau_c}$, and $\mathbb{E}_A(\cdot)$ is mathematical expectation with respect to A. Based on (11) and utilizing [31, (1.111)] and [31, (3.381.8)], $T_{2,k}^{\mathrm{TCCP}}$ is deduced as

$$\begin{aligned} T_{2,k}^{\mathrm{TCCP}} &= \mathbb{E}_{r_2}\left[\bar{F}_{\zeta_c}(b_4 r_2^{\alpha})\right] \\ &\quad - \mathbb{E}_{r_2}\left[\int_{b_4 r_2^{\alpha}}^{\infty}\bar{F}_{v_2}(b_1 y - b_2 r_2^{\alpha}) f_{\zeta_c}(y)\,dy\right] \\ &= \phi(b_4, 0, R) - \sum_{t=0}^{L-k-1}\sum_{n=0}^{t}\sum_{m=0}^{n}\chi_3 \\ &\quad\times\phi(b_1 b_4 + b_4 - b_2, \alpha(t-m), R), \end{aligned} \tag{41}$$

where $\phi(c,d,R) = \mathbb{E}_{r_2}\left[e^{-c r_2^{\alpha}} r_2^{d}\right]$ and $\chi_3 = \frac{{b_4}^{n-m}{b_1}^n(-b_2)^{t-n}}{(t-n)!(n-m)!(b_1+1)^{m+1}}$. Utilizing [31, (8.381.8)], we have $\phi(c,d,R) = \frac{2c^{-\frac{d+2}{\alpha}}}{R^2\alpha}\Upsilon\left(\frac{d+2}{\alpha}, cR^{\alpha}\right)$, where $\Upsilon(\cdot,\cdot)$ is lower

$$\begin{aligned}
P_{\mathrm{CP},1,k}^{\mathrm{TCCP}} &= \Pr\left\{\gamma_{c,1,k}^{\mathrm{TCCP}} > \Theta_{c,1}, \gamma_{p,1,k}^{\mathrm{TCCP}} > \Theta_{p,1}\right\} \\
&= \Pr\left\{v_1 < a_1\mu_{c,1} - a_2, v_1 > a_3\right\} \\
&= \Pr\left\{v_1 < a_1\mu_{c,1} - a_2, v_1 > a_3, \mu_{c,1} > \frac{a_2}{a_1}, a_1\mu_{c,1} - a_2 < a_3\right\} \\
&+ \Pr\left\{v_1 < a_1\mu_{c,1} - a_2, v_1 > a_3, \mu_{c,1} > \frac{a_2}{a_1}, a_1\mu_{c,1} - a_2 > a_3\right\} \\
&= \Pr\left\{a_3 < v_1 < a_1\mu_{c,1} - a_2, \mu_{c,1} > a_4\right\} \\
&= \underbrace{\int_{a_4}^{\infty} F_{v_1}\left(a_1 y - a_2\right) f_{\mu_{c,1}}\left(y\right) dy}_{\triangleq T_{1,k}^{\mathrm{TCCP}}} - \underbrace{F_{v_1}\left(a_3\right) \int_{a_4}^{\infty} f_{\mu_{c,1}}\left(y\right) dy}_{\triangleq V_{1,k}^{\mathrm{TCCP}}}
\end{aligned} \tag{37}$$

incomplete Gamma function defined by [31, (8.350.1)]. Similarly, we obtain

$$\begin{aligned}
V_{2,k}^{\mathrm{TCCP}} &= \mathbb{E}_{r_2}\left[F_{v_2}\left(b_3 r_2^{\alpha}\right) \bar{F}_{\zeta_c}\left(b_4 r_2^{\alpha}\right)\right] \\
&= \mathbb{E}_{r_2}\left[e^{-b_4 r_2^{\alpha}}\right] - \mathbb{E}_{r_2}\left[\sum_{t=0}^{L-k-1} \frac{b_3^t r_2^{\alpha t}}{t!} e^{-(b_3+b_4) r_2^{\alpha}}\right] \\
&= \phi\left(b_4, 0, R\right) - \sum_{t=0}^{L-k-1} \frac{1}{t!} b_3^t \phi\left(b_3 + b_4, \alpha t, R\right).
\end{aligned} \tag{42}$$

Appendix B
Proof of Lemma 2

Based on (13) and (14) and $\vartheta_1 = \mu_{c,1} + v_1$ [10], $P_{\mathrm{CP},1,k}^{\mathrm{TCAP}}$ is expressed as

$$\begin{aligned}
P_{\mathrm{CP},1,k}^{\mathrm{TCAP}} &= \Pr\left\{\frac{\delta_c \vartheta_1}{\delta_1 v_1 + 1} > \Theta_{c,1}, \delta_1 v_1 > \Theta_{p,1}\right\} \\
&= \Pr\left\{v_1 < a_1\vartheta_1 - a_2, v_1 > a_3\right\} \\
&= \Pr\left\{\left(1 - a_1\right) v_1 < a_1\mu_{c,1} - a_2, v_1 > a_3\right\}.
\end{aligned} \tag{43}$$

When $a_1 = 1$, we obtain

$$\begin{aligned}
P_{\mathrm{CP},1,k}^{\mathrm{TCAP}} &= \Pr\left\{\mu_{c,1} - a_2 > 0, v_1 > a_3\right\} \\
&= \bar{F}_{\mu_{c,1}}\left(a_2\right) \bar{F}_{v_1}\left(a_3\right).
\end{aligned} \tag{44}$$

When $a_1 < 1$, we have $\tau_c < \Theta_{c,1}\tau_1$, based on (10) and (11), and utilizing [31, (1.111)] and [31, (3.351.2)], we obtain

$$\begin{aligned}
P_{\mathrm{CP},1,k}^{\mathrm{TCAP}} &= \Pr\left\{\left(1 - a_1\right) v_1 < a_1\mu_{c,1} - a_2, v_1 > a_3, \mu_{c,1} > \frac{a_2}{a_1}\right\} \\
&= \Pr\left\{a_3 < v_1 < a_5\mu_{c,1} - a_6, \mu_{c,1} > \frac{a_2}{a_1}, \mu_{c,1} > a_7\right\} \\
&\overset{(c)}{=} \Pr\left\{a_3 < v_1 < a_5\mu_{c,1} - a_6, \mu_{c,1} > a_7\right\} \\
&= \int_{a_7}^{\infty} F_{v_1}\left(a_5 y - a_6\right) f_{\mu_{c,1}}\left(y\right) dy \\
&- F_{v_1}\left(a_3\right) \int_{a_7}^{\infty} f_{\mu_{c,1}}\left(y\right) dy \\
&= \bar{F}_{\mu_{c,1}}\left(a_7\right) \bar{F}_{v_1}\left(a_3\right) - I_0,
\end{aligned} \tag{45}$$

where $a_5 = \frac{a_1}{1-a_1}$, $a_6 = \frac{a_2}{1-a_1}$, $a_7 = \frac{a_3+a_6}{a_5} = \left(1 - a_1\right)\frac{a_3}{a_1} + \frac{a_2}{a_1} = \frac{(1+\Theta_{p,1})\Theta_{c,1}\delta_1 - \Theta_{p,1}\delta_c}{\delta_c\delta_1}$, $I_0 = \sum_{t=0}^{L-k-1} \frac{e^{a_6}}{(k-1)!t!} \int_{a_7}^{\infty} e^{-(a_5+1)y}(a_5 y - a_6)^t y^{k-1} dy = \sum_{t=0}^{L-k-1} \sum_{n=0}^{t} \chi_4\chi_5$, $\chi_4 = \frac{{a_5}^n(-a_6)^{t-n}e^{a_6}}{(t-n)!n!(k-1)!}$, $\chi_5 = \frac{\Gamma(n+k,(a_5+1)a_7)}{(a_5+1)^{n+k}}$, and step (c) is derived due to $a_7 > \frac{a_2}{a_1}$.

When $a_1 > 1$, we have $\tau_c > \Theta_{c,1}\tau_1$ and due to $a_7 < \frac{a_2}{a_1}$, $P_{\mathrm{CP},1,k}^{\mathrm{TCAP}}$ is obtained as

$$\begin{aligned}
P_{\mathrm{CP},1,k}^{\mathrm{TCAP}} &= \Pr\left\{\left(1 - a_1\right) v_1 < a_1\mu_{c,1} - a_2, v_1 > a_3\right\} \\
&= \Pr\left\{v_1 > a_3, v_1 > a_5\mu_{c,1} - a_6, \mu_{c,1} < \frac{a_2}{a_1}\right\} \\
&+ \Pr\left\{v_1 > a_3, \mu_{c,1} > \frac{a_2}{a_1}\right\} \\
&= \underbrace{\Pr\left\{v_1 > a_5\mu_{c,1} - a_6, \mu_{c,1} < a_7\right\}}_{\triangleq I_1} \\
&+ \underbrace{\Pr\left\{v_1 > a_3, \mu_{c,1} > a_7\right\}}_{\triangleq I_2}.
\end{aligned} \tag{46}$$

When $a_7 > 0$, we have $\frac{\tau_c}{\tau_1} < \frac{\Theta_{c,1}}{\Theta_{p,1}} + \Theta_{c,1}$, based on (10) and (11), utilizing [31, (3.351.1)], we derive

$$\begin{aligned}
I_1 &= \int_0^{a_7} \left(1 - F_{v_1}\left(a_5 y - a_6\right)\right) f_{\mu_{c,1}}\left(y\right) dy \\
&= \sum_{t=0}^{L-k-1} \frac{\int_0^{a_7} e^{-((a_5+1)y-a_6)}(a_5 y - a_6)^t y^{k-1} dy}{t!\left(k-1\right)!} \\
&= \sum_{t=0}^{L-k-1} \frac{\int_{-a_6}^{(a_5+1)a_7-a_6} e^{-x}(a_5 x - a_6)^t (x + a_6)^{k-1} dx}{t!\left(k-1\right)!(a_5+1)^{t+k}} \\
&= \sum_{t=0}^{L-k-1} \sum_{n=0}^{t} \sum_{m=0}^{k-1} \chi_6 \int_{-a_6}^{(a_5+1)a_7-a_6} x^{n+m} e^{-x} dx \\
&= \sum_{t=0}^{L-k-1} \sum_{n=0}^{t} \sum_{m=0}^{k-1} \chi_6\chi_7,
\end{aligned} \tag{47}$$

where $\chi_6 = \frac{(-1)^{t-n}a_5^n a_6^{t+k-n-m-1}}{(a_5+1)^{t+k}(k-m-1)!(t-n)!n!m!}$ and $\chi_7 = \Upsilon\left(n+m+1, \left(a_5+1\right)a_7 - a_6\right) - \Upsilon\left(n+m+1, -a_6\right)$. Similarly, we derive $I_2 = \bar{F}_{v_1}\left(a_3\right)\bar{F}_{\mu_{c,1}}\left(a_7\right)$. For $a_7 \leq 0$, we have $\frac{\tau_c}{\tau_1} > \frac{\Theta_{c,1}}{\Theta_{p,1}} + \Theta_{c,1}$, with the same method as utilized for (47), we obtain $I_1 = 0$ and

$$P_{\mathrm{CP},1,k}^{\mathrm{TCAP}} = I_2 = \Pr\left\{v_1 > a_3\right\} = \bar{F}_{v_1}\left(a_3\right). \tag{48}$$

$$
\begin{aligned}
P_{\mathrm{CP},2,k}^{\mathrm{TCAP}} &= \Pr\left\{(1-b_1)\,v_2 < b_1\mu_{c,2} - b_2 r_2^{\alpha}, v_2 > b_3 r_2^{\alpha}, b_1\mu_{c,2} - b_2 r_2^{\alpha} > 0\right\} \\
&= \Pr\left\{v_2 < b_5\mu_{c,2} - b_6 r_2^{\alpha}, v_2 > b_3 r_2^{\alpha}, \mu_{c,2} > \frac{b_2 r_2^{\alpha}}{b_1}\right\} \\
&= \Pr\left\{v_2 < b_5\mu_{c,2} - b_6 r_2^{\alpha}, v_2 > b_3 r_2^{\alpha}, \mu_{c,2} > \frac{b_2 r_2^{\alpha}}{b_1}, b_5\mu_{c,2} - b_6 r_2^{\alpha} > b_3 r_2^{\alpha}\right\} \\
&+ \Pr\left\{v_2 < b_5\mu_{c,2} - b_6 r_2^{\alpha}, v_2 > b_3 r_2^{\alpha}, \mu_{c,2} > \frac{b_2 r_2^{\alpha}}{b_1}, b_5\mu_{c,2} - b_6 r_2^{\alpha} < b_3 r_2^{\alpha}\right\} \\
&\overset{(d)}{=} \Pr\left\{b_3 r_2^{\alpha} < v_2 < b_5\mu_{c,2} - b_6 r_2^{\alpha}, \mu_{c,2} > b_7 r_2^{\alpha}\right\} \\
&= \underbrace{\mathbb{E}_{r_2}\left[\int_{b_7 r_2^{\alpha}}^{\infty} F_{v_2}\left(b_5 y - b_6 r_2^{\alpha}\right) f_{\mu_{c,2}}(y)\,dy\right]}_{\triangleq I_3} - \underbrace{\mathbb{E}_{r_2}\left[F_{v_2}\left(b_3 r_2^{\alpha}\right)\int_{b_7 r_2^{\alpha}}^{\infty} f_{\mu_{c,2}}(y)\,dy\right]}_{\triangleq I_4}
\end{aligned}
\tag{51}
$$

Appendix C
Proof of Lemma 3

Utilizing same method as for (43), $P_{\mathrm{CP},2,k}^{\mathrm{TCAP}}$ is denoted as

$$
\begin{aligned}
P_{\mathrm{CP},2,k}^{\mathrm{TCAP}} &= \Pr\left\{v_2 < b_1\left(v_2 + \mu_{c,2}\right) - b_2 r_2^{\alpha}, v_2 > b_3 r_2^{\alpha}\right\} \\
&= \Pr\left\{(1-b_1)\,v_2 < b_1\mu_{c,2} - b_2 r_2^{\alpha}, v_2 > b_3 r_2^{\alpha}\right\}.
\end{aligned}
\tag{49}
$$

When $b_1 = 1$, based on (10) and (11), we obtain

$$
\begin{aligned}
P_{\mathrm{CP},2,k}^{\mathrm{TCAP}} &= \Pr\left\{\mu_{c,2} - b_2 r_2^{\alpha} > 0, v_2 > b_3 r_2^{\alpha}\right\} \\
&= \mathbb{E}_{r_2}\left[\bar{F}_{\mu_{c,2}}\left(b_2 r_2^{\alpha}\right)\bar{F}_{v_2}\left(b_3 r_2^{\alpha}\right)\right] \\
&= \sum_{t=0}^{L-k-1}\sum_{n=0}^{k-1}\frac{b_3^t b_2^n}{t!n!}\mathbb{E}_{r_2}\left[e^{-(b_3+b_2)r_2^{\alpha}} r_2^{\alpha(t+n)}\right] \\
&= \sum_{t=0}^{L-k-1}\sum_{n=0}^{k-1}\frac{b_3^t b_2^n}{t!n!}\phi\left(b_3 + b_2, \alpha\left(t+n\right), R\right).
\end{aligned}
\tag{50}
$$

When $b_1 < 1$, we have $\tau_c < \Theta_{c,2}\tau_2$, thus $P_{\mathrm{CP},2,k}^{\mathrm{TCAP}}$ is expressed as (51), shown at the top of this page, where $b_5 = \frac{b_1}{1-b_1}$, $b_6 = \frac{b_2}{1-b_1}$ $b_7 = \frac{(1-b_1)b_3+b_2}{b_1} = \frac{(\Theta_{c,2}\tau_2-\tau_c)\Theta_{\mathrm{p},2}+\Theta_{c,2}\tau_2}{\delta\tau_2\tau_c}$, and step (d) is derived from $b_7 > \frac{b_2}{b_1}$. Subsequently, substituting (10) and (11) into (51), we obtain

$$
\begin{aligned}
I_3 &= \mathbb{E}_{r_2}\left[\int_{b_7 r_2^{\alpha}}^{\infty} F_{v_2}\left(b_5 y - b_6 r_2^{\alpha}\right) f_{\mu_{c,2}}(y)\,dy\right] \\
&= \mathbb{E}_{r_2}\left[\bar{F}_{\mu_{c,2}}\left(b_7 r_2^{\alpha}\right)\right] \\
&- \mathbb{E}_{r_2}\left[\int_{b_7 r_2^{\alpha}}^{\infty} \bar{F}_{v_2}\left(b_5 y - b_6 r_2^{\alpha}\right) f_{\mu_{c,2}}(y)\,dy\right] \\
&= \sum_{t=0}^{k-1}\frac{b_7^t}{t!}\mathbb{E}_{r_2}\left[e^{-b_7 r_2^{\alpha}} r_2^{\alpha t}\right] - \sum_{t=0}^{L-k-1}\sum_{m=0}^{t}\chi_8\chi_9 \\
&= \sum_{t=0}^{k-1}\frac{b_7^t}{t!}\phi\left(b_7, \alpha t, R\right) - \sum_{t=0}^{L-k-1}\sum_{m=0}^{t}\chi_8\chi_9,
\end{aligned}
\tag{52}
$$

where $\chi_8 = \frac{b_5^m(-b_6)^{t-m}}{(t-m)!m!(k-1)!}$, χ_9 is obtained as

$$
\begin{aligned}
\chi_9 &= \mathbb{E}_{r_2}\left[e^{b_6 r_2^{\alpha}} r_2^{\alpha(t-m)}\int_{b_7 r_2^{\alpha}}^{\infty} e^{-(b_5+1)y} y^{k+m-1} dy\right] \\
&\overset{(e)}{=} \frac{\mathbb{E}_{r_2}\left[e^{b_6 r_2^{\alpha}} r_2^{\alpha(t-m)}\Gamma\left(k+m, \left(b_5+1\right) b_7 r_2^{\alpha}\right)\right]}{\left(b_5+1\right)^{k+m}} \\
&\overset{(f)}{=} \sum_{z=0}^{k+m-1}\frac{b_7^z\left(k+m-1\right)!}{z!\left(b_5+1\right)^{k+m-z}} \\
&\times \phi\left(b_5 b_7 + b_7 - b_6, \alpha\left(t-m+z\right), R\right),
\end{aligned}
\tag{53}
$$

where step (e) is obtained by invoking [31, (3.351.2)] and step (f) is obtained by invoking [31, (8.352.2)]. Utilizing the same method as for I_3, I_4 is obtained as

$$
\begin{aligned}
I_4 &= \mathbb{E}_{r_2}\left[F_{v_2}\left(b_3 r_2^{\alpha}\right)\bar{F}_{\mu_{c,2}}\left(b_7 r_2^{\alpha}\right)\right] \\
&= \sum_{n=0}^{k-1}\frac{b_7^n}{n!}\left(\mathbb{E}_{r_2}\left[e^{-b_7 r_2^{\alpha}} r_2^{\alpha n}\right]\right. \\
&\left. - \sum_{t=0}^{L-k-1}\frac{b_3^t}{t!}\mathbb{E}_{r_2}\left[e^{-(b_3+b_7)r_2^{\alpha}} r_2^{\alpha(t+n)}\right]\right) \\
&= \sum_{n=0}^{k-1}\frac{b_7^n}{n!}\left(\phi\left(b_7, \alpha n, R\right)\right. \\
&\left. - \sum_{t=0}^{L-k-1}\frac{b_3^t}{t!}\phi\left(b_3 + b_7, \alpha\left(t+n\right), R\right)\right).
\end{aligned}
\tag{54}
$$

When $b_1 > 1$, we have $\tau_c > \Theta_{c,2}\tau_2$ and due to $b_7 < \frac{b_2}{b_1}$, we express $P_{\mathrm{CP},2,k}^{\mathrm{TCAP}}$ as (55), shown at the top of next page.

Similar to (47), when $b_7 > 0$, we have $\frac{\tau_c}{\tau_2} < \frac{\Theta_{c,2}}{\Theta_{\mathrm{p},2}} + \Theta_{c,2}$, based on (10) and (11), and utilizing [31, (3.351.1), (8.352.1)], we obtain

$$
\begin{aligned}
I_5 &= \Pr\left\{\mu_{c,2} > b_7 r_2^{\alpha}, v_2 > b_3 r_2^{\alpha}\right\} \\
&= \mathbb{E}_{r_2}\left[\bar{F}_{v_2}\left(b_3 r_2^{\alpha}\right)\bar{F}_{\mu_{c,2}}\left(b_7 r_2^{\alpha}\right)\right] \\
&= \sum_{t=0}^{L-k-1}\sum_{n=0}^{k-1}\frac{b_3^t b_7^n}{t!n!}\mathbb{E}_{r_2}\left[e^{-(b_3+b_7)r_2^{\alpha}} r_2^{\alpha(t+n)}\right] \\
&= \sum_{t=0}^{L-k-1}\sum_{n=0}^{k-1}\frac{b_3^t b_7^n}{t!n!}\phi\left(b_3 + b_7, \alpha\left(t+n\right), R\right).
\end{aligned}
\tag{56}
$$

$$
\begin{aligned}
P_{\mathrm{CP},2,k}^{\mathrm{TCAP}} &= \Pr\left\{(1-b_1)\,v_2 < b_1\mu_{c,2} - b_2 r_2^{\alpha}, v_2 > b_3 r_2^{\alpha}, b_1\mu_{c,2} - b_2 r_2^{\alpha} < 0\right\} \\
&+ \Pr\left\{(1-b_1)\,v_2 < b_1\mu_{c,2} - b_2 r_2^{\alpha}, v_2 > b_3 r_2^{\alpha}, b_1\mu_{c,2} - b_2 r_2^{\alpha} > 0\right\} \\
&= \Pr\left\{\mu_{c,2} > \frac{b_2 r_2^{\alpha}}{b_1}, v_2 > b_3 r_2^{\alpha}\right\} + \Pr\left\{\mu_{c,2} < \frac{b_2 r_2^{\alpha}}{b_1}, b_5\mu_{c,2} - b_6 r_2^{\alpha} < b_3 r_2^{\alpha}, v_2 > b_3 r_2^{\alpha}\right\} \\
&+ \Pr\left\{\mu_{c,2} < \frac{b_2 r_2^{\alpha}}{b_1}, b_5\mu_{c,2} - b_6 r_2^{\alpha} > b_3 r_2^{\alpha}, v_2 > b_5\mu_{c,2} - b_6 r_2^{\alpha}\right\} \\
&= \Pr\left\{\mu_{c,2} > \frac{b_2 r_2^{\alpha}}{b_1}, v_2 > b_3 r_2^{\alpha}\right\} + \Pr\left\{\mu_{c,2} < \frac{b_2 r_2^{\alpha}}{b_1}, \mu_{c,2} > b_7 r_2^{\alpha}, v_2 > b_3 r_2^{\alpha}\right\} \\
&+ \Pr\left\{\mu_{c,2} < \frac{b_2 r_2^{\alpha}}{b_1}, \mu_{c,2} < b_7 r_2^{\alpha}, v_2 > b_5\mu_{c,2} - b_6 r_2^{\alpha}\right\} \\
&= \underbrace{\Pr\left\{b_7 r_2^{\alpha} < \mu_{c,2}, v_2 > b_3 r_2^{\alpha}\right\}}_{\triangleq I_5} + \underbrace{\Pr\left\{\mu_{c,2} < b_7 r_2^{\alpha}, v_2 > b_5\mu_{c,2} - b_6 r_2^{\alpha}\right\}}_{\triangleq I_6}
\end{aligned}
\tag{55}
$$

Utilizing same method as I_2, we obtain

$$
\begin{aligned}
I_6 &= \Pr\left\{\mu_{c,2} < b_7 r_2^{\alpha}, v_2 > b_5\mu_{c,2} - b_6 r_2^{\alpha}\right\} \\
&= \mathbb{E}\left[\int_0^{b_7 r_2^{\alpha}} \left(1 - F_{v_1}\left(b_5 y - b_6 r_2^{\alpha}\right)\right) f_{\mu_{c,2}}(y)\, dy\right] \\
&= \frac{1}{(k-1)!}\sum_{t=0}^{L-k-1}\frac{1}{t!}\mathbb{E}_{r_2}\left[\int_{-b_6 r_2^{\alpha}}^{(b_5 b_7 + b_7 - b_6) r_2^{\alpha}} e^{-x}\right. \\
&\left.\times\left(\frac{b_5 x - b_6 r_2^{\alpha}}{b_5+1}\right)^t\left(\frac{x + b_6 r_2^{\alpha}}{b_5+1}\right)^{k-1}\frac{dx}{b_5+1}\right] \\
&= \sum_{t=0}^{L-k-1}\sum_{n=0}^{k-1}\sum_{m=0}^{t}\chi_{10}\chi_{11},
\end{aligned}
\tag{57}
$$

where $\chi_{10} = \frac{b_5^m (-b_6)^{t-m} b_6^{k-n-1}}{(k-n-1)!(t-m)!m!n!(b_5+1)^{t+k}}$ and $\chi_{11} = \mathbb{E}_{r_2}\left[r_2^{\alpha(t-n+k-m-1)}\int_{-b_6 r_2^{\alpha}}^{(b_5 b_7 + b_7 - b_6) r_2^{\alpha}} e^{-x} x^{n+m} dx\right]$. Utilizing same method as I_2, χ_{11} is obtained as

$$
\begin{aligned}
\chi_{11} &= \mathbb{E}_{r_2}\left[\frac{\Upsilon\left(n+m+1, (b_5 b_7 + b_7 - b_6)\, r_2^{\alpha}\right)}{r_2^{-\alpha(t-n+k-m-1)}}\right] \\
&- \mathbb{E}_{r_2}\left[r_2^{\alpha(t-n+k-m-1)}\Upsilon\left(n+m+1, -b_6 r_2^{\alpha}\right)\right] \\
&= \sum_{z=0}^{n+m}\left(\frac{(n+m)!}{z!(-b_6)^{-z}}\mathbb{E}\left[e^{b_6 r_2^{\alpha}} r_2^{\alpha(t-n+k-m-1+z)}\right]\right. \\
&\left.-\frac{(n+m)!}{z!(b_5 b_7 + b_7 - b_6)^{-z}}\mathbb{E}\left[\frac{r_2^{\alpha(t-n+k-m-1+z)}}{e^{(b_5 b_7 + b_7 - b_6) r_2^{\alpha}}}\right]\right) \\
&= \sum_{z=0}^{n+m}\left(\chi_{12} - \chi_{13}\right),
\end{aligned}
\tag{58}
$$

where $\chi_{12} = \frac{(n+m)!\phi(-b_6, \alpha(t-n+k-m-1+z), R)}{z!(-b_6)^{-z}}$ and $\chi_{13} = \frac{(n+m)!\phi(b_5 b_7 + b_7 - b_6, \alpha(t-n+k-m-1+z), R)}{z!(b_5 b_7 + b_7 - b_6)^{-z}}$.

When $b_7 \le 0$, we have $\frac{\tau_c}{\tau_2} \ge \frac{\Theta_{c,2}}{\Theta_{\mathrm{p},2}} + \Theta_{c,2}$, thus, we obtain $I_6 = 0$. Based on (11), $P_{\mathrm{CP},2,k}^{\mathrm{TCAP}}$ with $0 < k < L$ is obtained as

$$
\begin{aligned}
P_{\mathrm{CP},2,k}^{\mathrm{TCAP}} &= I_5 = \Pr\left\{v_2 > b_3 r_2^{\alpha}\right\} \\
&= \mathbb{E}_{r_2}\left[\bar{F}_{v_2}\left(b_3 r_2^{\alpha}\right)\right] \\
&= \sum_{t=0}^{L-k-1}\frac{b_3^t}{t!}\phi\left(b_3, \alpha t, R\right).
\end{aligned}
\tag{59}
$$

Appendix D
Proof of Theorem 3

Based on $\sum_{t=0}^{n-1}\frac{x^t}{t!} = e^x - \frac{x^n}{n!} + O\left(x^n\right)$, we obtain $F_X(x) = \frac{x^{\kappa_X}}{\kappa_X!} + \mathcal{O}\left(x^{\kappa_X}\right)$ when $x \to 0$. When $\rho \to \infty$, we have $a_2 \to 0$, $a_3 \to 0$, and $a_4 \to 0$.

Based on (38), by utilizing $\Gamma(n, x) \overset{x\to 0}{\approx} \Gamma(n) - \frac{x^n}{n}$, $T_{1,k}^{\mathrm{TCCP},\infty}$ and invoking [31, (3.351.2)], $T_{1,k}^{\mathrm{TCCP},\infty}$ with $0 < k < L$ is obtained as

$$
\begin{aligned}
T_{1,k}^{\mathrm{TCCP},\infty} &= \int_{a_4}^{\infty} F_{v_1}\left(a_1 y\right) f_{\mu_{c,1}}(y)\, dy \\
&= \bar{F}_{\mu_{c,1}}\left(a_4\right) - \sum_{t=0}^{L-k-1}\frac{a_1^t}{(k-1)!t!} \\
&\times\int_{a_4}^{\infty} e^{-(a_1+1)y} y^{t+k-1} dy \\
&= 1 - \frac{a_4^k}{k!} - \sum_{t=0}^{L-k-1}\frac{a_1^t\Gamma\left(t+k, (a_1+1)\, a_4\right)}{(a_1+1)^{t+k}(k-1)!t!} \\
&\approx 1 - \frac{a_4^k}{k!} + \sum_{t=0}^{L-k-1}\frac{a_1^t}{(k-1)!t!} \\
&\times\left(\frac{a_4^{t+k}}{t+k} - \frac{(t+k-1)!}{(a_1+1)^{t+k}}\right).
\end{aligned}
\tag{60}
$$

Similarly, by utilizing $F_X(x) = \frac{x^{\kappa_X}}{\kappa_X!} + \mathcal{O}\left(x^{\kappa_X}\right)$, $V_{1,k}^{\mathrm{TCCP},\infty}$ with $0 < k < L$ is obtained as

$$
\begin{aligned}
&V_{1,k}^{\mathrm{TCCP},\infty} \\
&= F_{v_1}^{\infty}\left(a_3\right)\left(1 - F_{\mu_c}^{\infty}\left(a_4\right)\right) \\
&= \frac{{a_3}^{L-k}}{(L-k)!}\left(1 - \frac{a_4^k}{k!}\right).
\end{aligned}
\tag{61}
$$

Based on (19) and (21), we obtain $P_{\mathrm{out},1,0}^{\mathrm{TCCP},\infty} = \frac{1}{L!}\left(\frac{r_1^{\alpha}\Theta_{p,1}}{\delta\tau_1}\right)^L$ and $P_{\mathrm{out},1,L}^{\mathrm{TCCP},\infty} = \frac{1}{L!}\left(\frac{r_1^{\alpha}\Theta_{c,1}}{\delta}\right)^L$. Subsequently, based on (60) and (61), and combining the aforementioned

results of $P_{\text{out},1,0}^{\text{TCCP},\infty}$ and $P_{\text{out},1,L}^{\text{TCCP},\infty}$, $P_{\text{out},1}^{\text{TCCP},\infty}$ is obtained as

$$\begin{aligned}P_{\text{out},1}^{\text{TCCP},\infty} &= \frac{1}{L!}\left(\omega_0\left(\frac{\Theta_{p,1}r_1^{\alpha}}{\delta\tau_1}\right)^L + \omega_L\left(\frac{\Theta_{c,1}r_1^{\alpha}}{\delta}\right)^L\right)\\ &+ \sum_{k=1}^{L-1}\left(\frac{\omega_k {a_3}^{L-k}}{(L-k)!} + \frac{\omega_k a_4^k}{k!}\left(1-\frac{{a_3}^{L-k}}{(L-k)!}\right)\right)\\ &- \sum_{k=1}^{L-1}\sum_{t=0}^{L-k-1}\left(\frac{\omega_k a_1^t a_4^{t+k}}{(k-1)!t!\,(t+k)}\right.\\ &\left.- \frac{\omega_k a_1^t\,(t+k-1)!}{(k-1)!t!(a_1+1)^{t+k}}\right)\\ &\overset{(g)}{\approx} \sum_{k=1}^{L-1}\sum_{t=0}^{L-k-1}\frac{\omega_k a_1^t\,(t+k-1)!}{(k-1)!t!(a_1+1)^{t+k}},\end{aligned} \tag{62}$$

where step (g) is due to $\delta\to\infty$, $a_3\to 0$, and $a_4\to 0$.

Similar to (60), we have $b_2\to 0$, $b_3\to 0$, and $b_4\to 0$ when $\rho\to\infty$. Based on $1-e^{-y}\overset{y\to 0}{\approx} y$, we obtain $F_Y^{\infty}(y)=y$. Based on (41), by utilizing $\Upsilon(n,x)\overset{x\to 0}{\approx}\frac{x^n}{n}$, $T_{2,k}^{\text{TCCP},\infty}$ with $0<k<L$ is obtained as

$$\begin{aligned}&T_{2,k}^{\text{TCCP},\infty}\\ &= \mathbb{E}_{r_2}\left[\bar{F}_{\zeta_c}^{\infty}(b_4 r_2^{\alpha})\right]\\ &- \mathbb{E}_{r_2}\left[\int_{b_4 r_2^{\alpha}}^{\infty}\bar{F}_{v_2}(b_1 y - b_2 r_2^{\alpha}) f_{\zeta_c}(y)\,dy\right]\\ &= \mathbb{E}_{r_2}\left[1-b_4 r_2^{\alpha}\right]\\ &- \sum_{t=0}^{L-k-1}\sum_{n=0}^{t}\sum_{m=0}^{n}\frac{2\chi_3}{\alpha R^2}\frac{\Upsilon\left(t-m+\frac{2}{\alpha},(b_1b_4+b_4-b_2)R^{\alpha}\right)}{(b_1b_4+b_4-b_2)^{t-m+\frac{2}{\alpha}}}\\ &\approx 1-\frac{2b_4R^{\alpha}}{\alpha+2}-\sum_{t=0}^{L-k-1}\sum_{n=0}^{t}\sum_{m=0}^{n}\frac{2\chi_3 R^{\alpha(t-m)}}{\alpha(t-m)+2}.\end{aligned} \tag{63}$$

Similarly, by utilizing $F_X(x)=\frac{x^{\kappa_X}}{\kappa_X!}+\mathcal{O}(x^{\kappa_X})$, $V_{2,k}^{\text{TCCP},\infty}$ with $0<k<L$ is obtained as

$$\begin{aligned}&V_{2,k}^{\text{TCCP},\infty}\\ &= \mathbb{E}_{r_2}\left[F_{v_2}^{\infty}(b_3 r_2^{\alpha})\,\bar{F}_{\zeta_c}^{\infty}(b_4 r_2^{\alpha})\right]\\ &= \mathbb{E}_{r_2}\left[\frac{b_3^{L-k}r_2^{\alpha(L-k)}}{(L-k)!}(1-b_4 r_2^{\alpha})\right]\\ &= \frac{b_3^{L-k}}{(L-k)!}\left(\mathbb{E}_{r_2}\left[r_2^{\alpha(L-k)}\right]-b_4\mathbb{E}_{r_2}\left[r_2^{\alpha(L-k+1)}\right]\right)\\ &= \frac{2b_3^{L-k}}{(L-k)!}\left(\frac{R^{\alpha(L-k)}}{\alpha(L-k)+2}\right.\\ &\left.-\frac{b_4R^{\alpha(L-k+1)}}{\alpha(L-k+1)+2}\right).\end{aligned} \tag{64}$$

Similarly, based on (20) and (22), we obtain $P_{\text{out},2,0}^{\text{TCCP},\infty}=\mathbb{E}_{r_2}\left[F_{\vartheta_2}^{\infty}\left(\frac{\Theta_{p,2}}{\delta\tau_2}r_2^{\alpha}\right)\right]=\frac{2R^{\alpha L}{\Theta_{p,2}}^L}{L!(\alpha L+2)(\delta\tau_2)^L}$ and $P_{\text{out},2,L}^{\text{TCCP},\infty}=\mathbb{E}_{r_2}\left[F_{\zeta}^{\infty}\left(\frac{r_2^{\alpha}\Theta_{c,2}}{\delta}\right)\right]=\mathbb{E}_{r_2}\left[\frac{r_2^{\alpha}\Theta_{c,2}}{\delta\tau_2}\right]=\frac{2\Theta_{c,2}R^{\alpha}}{(\alpha+2)\delta\tau_2}$.

Finally, $P_{\text{out},2}^{\text{TCCP},\infty}$ is obtained as (65), shown at the top of next page. where step (h) is due to $\delta\to\infty$, $b_3\to 0$, $b_4\to 0$ and step (i) is due to $\chi_3\neq 0$ only if $t=n=m$ with $b_2\to 0$ and $b_4\to 0$.

Appendix E
Proof of Theorem 4

Since $P_{\text{out},1,0}^{\text{TCAP}}=P_{\text{out},1,0}^{\text{TCCP}}$ and $P_{\text{out},1,L}^{\text{TCAP}}=P_{\text{out},1,L}^{\text{TCCP}}$, $P_{\text{out},1}^{\text{TCAP},\infty}$ is obtained as

$$\begin{aligned}P_{\text{out},1}^{\text{TCAP},\infty} &= \frac{\omega_0}{L!}\left(\frac{\Theta_{p,1}r_1^{\alpha}}{\delta\tau_1}\right)^L+\frac{\omega_L}{L!}\left(\frac{\Theta_{c,1}r_1^{\alpha}}{\delta}\right)^L\\ &+\sum_{k=1}^{L-1}\omega_k\left(1-P_{\text{CP},1,k}^{\text{TCAP},\infty}\right).\end{aligned} \tag{66}$$

When $\rho\to\infty$, we have $a_2\to 0$ and $a_3\to 0$. Thus, for $0<k<L$, when $a_1=1$, based on (44), we obtain

$$\begin{aligned}P_{\text{CP},1,k}^{\text{TCAP},\infty} &= \bar{F}_{\mu_{c,1}}^{\infty}(a_2)\,\bar{F}_{v_1}^{\infty}(a_3)\\ &= 1-\frac{a_2^k}{k!}-\frac{a_3^{L-k}}{(L-k)!}+\frac{a_2^k a_3^{L-k}}{k!\,(L-k)!}.\end{aligned} \tag{67}$$

Then, $P_{\text{out},1}^{\text{TCAP},\infty}$ with $a_1=1$ is obtained as

$$\begin{aligned}P_{\text{out},1}^{\text{TCAP},\infty} &= \frac{\omega_0}{L!}\left(\frac{\Theta_{p,1}r_1^{\alpha}}{\delta\tau_1}\right)^L+\frac{\omega_L}{L!}\left(\frac{\Theta_{c,1}r_1^{\alpha}}{\delta}\right)^L\\ &+\sum_{k=1}^{L-1}\left(\frac{\omega_k a_2^k}{k!}+\frac{\omega_k a_3^{L-k}}{(L-k)!}-\frac{\omega_k a_2^k a_3^{L-k}}{k!\,(L-k)!}\right)\\ &\approx \sum_{k=1}^{L-1}\left(\frac{\omega_k a_2^k}{k!}+\frac{\omega_k a_3^{L-k}}{(L-k)!}\right)\\ &\approx \omega_1 a_2+\omega_{L-1}a_3.\end{aligned} \tag{68}$$

For $a_1<1$, based on (45), we obtain $P_{\text{CP},1,k}^{\text{TCAP},\infty}$ as

$$\begin{aligned}P_{\text{CP},1,k}^{\text{TCAP},\infty} &= \bar{F}_{\mu_{c,1}}^{\infty}(a_7)\,\bar{F}_{v_1}^{\infty}(a_3)-\sum_{t=0}^{L-k-1}\frac{a_5^t}{(k-1)!t!}\\ &\times\int_{a_7}^{\infty}e^{-(a_5+1)y}y^{t+k-1}dy\\ &\approx 1-\frac{a_7^k}{k!}-\frac{a_3^{L-k}}{(L-k)!}\\ &-\sum_{t=0}^{L-k-1}\frac{a_5^t(a_5+1)^{-t-k}}{(k-1)!t!}\Gamma(t+k,(a_5+1)a_7)\\ &\approx 1-\frac{a_7^k}{k!}-\frac{a_3^{L-k}}{(L-k)!}\\ &+\sum_{t=0}^{L-k-1}\frac{a_5^t}{(k-1)!t!}\left(\frac{a_7^{t+k}}{t+k}-\frac{(t+k-1)!}{(a_5+1)^{t+k}}\right)\\ &\approx 1-\frac{a_3^{L-k}}{(L-k)!}-\sum_{t=0}^{L-k-1}\frac{a_5^t\,(t+k-1)!}{(k-1)!t!(a_5+1)^{t+k}}.\end{aligned} \tag{69}$$

Then, by substituting (69) into (66), $P_{\text{out},1}^{\text{TCAP},\infty}$ for $a_1<1$ is obtained as

$$\begin{aligned}P_{\text{out},1}^{\text{TCAP},\infty} &= \frac{\omega_0}{L!}\left(\frac{\Theta_{p,1}r_1^{\alpha}}{\delta\tau_1}\right)^L+\frac{\omega_L}{L!}\left(\frac{\Theta_{c,1}r_1^{\alpha}}{\delta}\right)^L\\ &+\sum_{k=1}^{L-1}\left(\frac{\omega_k a_3^{L-k}}{(L-k)!}+\sum_{t=0}^{L-k-1}\frac{\omega_k a_5^t\,(t+k-1)!}{(k-1)!t!(a_5+1)^{t+k}}\right)\\ &\approx \sum_{k=1}^{L-1}\sum_{t=0}^{L-k-1}\frac{\omega_k a_5^t\,(t+k-1)!}{(k-1)!t!(a_5+1)^{t+k}}.\end{aligned} \tag{70}$$

$$P_{\text{out},2}^{\text{TCCP},\infty}=\frac{2\omega_0R^{\alpha L}\Theta_{p,2}^L}{L!\left(\alpha L+2\right)\left(\delta\tau_2\right)^L}+\frac{2\omega_LR^{\alpha}\Theta_{c,2}}{\left(\alpha+2\right)\delta\tau_2}+\sum_{k=1}^{L-1}\sum_{t=0}^{L-k-1}\sum_{n=0}^{t}\sum_{m=0}^{n}\frac{2\omega_k\chi_3R^{\alpha(t-m)}}{\alpha\left(t-m\right)+2}$$
$$+\sum_{k=1}^{L-1}\left(\frac{2\omega_kb_4R^{\alpha}}{\alpha+2}+\frac{2\omega_kb_3^{L-k}R^{\alpha(L-k)}}{(L-k)!}\left(\frac{1}{\alpha\left(L-k\right)+2}-\frac{b_4R^{\alpha}}{\alpha\left(L-k+1\right)+2}\right)\right)$$
$$\overset{(h)}{\approx}\sum_{k=1}^{L-1}\sum_{t=0}^{L-k-1}\sum_{n=0}^{t}\sum_{m=0}^{n}\frac{2\omega_k\chi_3R^{\alpha(t-m)}}{\alpha\left(t-m\right)+2}\overset{(i)}{\approx}\sum_{k=1}^{L-1}\sum_{t=0}^{L-k-1}\frac{\omega_k{b_1}^t}{\left(b_1+1\right)^{t+1}} \tag{65}$$

For $a_1>1$ and $a_7>0$, based on (46), by utilizing $\Upsilon\left(n,x\right)\overset{x\to0}{\approx}\frac{x^n}{n}$, $P_{\text{CP},1,k}^{\text{TCAP},\infty}$ is obtained as

$$\begin{aligned}P_{\text{CP},1,k}^{\text{TCAP},\infty}&=I_1^{\infty}+I_2^{\infty}=\int_0^{a_7}\left(1-F_{v_1}\left(a_5y\right)\right)f_{\mu_{c,1}}\left(y\right)dy\\&+\bar{F}_{v_1}^{\infty}\left(a_3\right)\bar{F}_{\mu_{c,1}}^{\infty}\left(a_7\right)\\&=\sum_{t=0}^{L-k-1}\frac{a_5^t(a_5+1)^{-(t+k)}}{t!\left(k-1\right)!}\Upsilon\left(t+k,\left(a_5+1\right)a_7\right)\\&+1-\frac{a_7^k}{k!}-\frac{a_3^{L-k}}{(L-k)!}+\frac{a_7^ka_3^{L-k}}{k!\left(L-k\right)!}\\&\approx\sum_{t=0}^{L-k-1}\frac{a_5^ta_7^{t+k}}{t!\left(k-1\right)!\left(t+k\right)}+1-\frac{a_7^k}{k!}-\frac{a_3^{L-k}}{(L-k)!}\\&\approx1-\frac{a_3^{L-k}}{(L-k)!}.\end{aligned} \tag{71}$$

For $a_1>1$ and $a_7\leq0$, based on (48), we have $P_{\text{CP},1,k}^{\text{TCAP},\infty}=I_2^{\infty}=\bar{F}_{v_1}^{\infty}\left(a_3\right)=1-\frac{a_3^{L-k}}{(L-k)!}$. Then, $P_{\text{CP},1,k}^{\text{TCAP},\infty}$ for $a_1>1$ is obtained as

$$P_{\text{CP},1,k}^{\text{TCAP},\infty}=1-\frac{a_3^{L-k}}{(L-k)!}. \tag{72}$$

Finally, $P_{\text{out},1}^{\text{TCAP},\infty}$ for $a_1>1$ is obtained as

$$P_{\text{out},1}^{\text{TCAP},\infty}=\sum_{k=1}^{L-1}\frac{\omega_ka_3^{L-k}}{(L-k)!}\approx\omega_{L-1}a_3. \tag{73}$$

Based on (20) and (27), we have $P_{\text{out},2,L}^{\text{TCAP}}=\mathbb{E}_{r_2}\left[F_{\vartheta_2}^{\infty}\left(\frac{\Theta_{c,2}}{\delta}r_2^{\alpha}\right)\right]=\frac{1}{L!}\left(\frac{\Theta_{c,2}}{\delta}\right)^L\mathbb{E}_{r_2}\left[r_2^{\alpha L}\right]=\frac{2R^{\alpha L}\Theta_{c,2}^L}{L!(\alpha L+2)\delta^L}$, $P_{\text{out},2,0}^{\text{TCCP},\infty}=\mathbb{E}_{r_2}\left[F_{\vartheta_2}^{\infty}\left(\frac{\Theta_{p,2}}{\delta\tau_2}r_2^{\alpha}\right)\right]=\frac{1}{L!}\left(\frac{\Theta_{p,2}}{\delta\tau_2}\right)^L\mathbb{E}_{r_2}\left[r_2^{\alpha L}\right]=\frac{2R^{\alpha L}\Theta_{p,2}^L}{L!(\alpha L+2)(\delta\tau_2)^L}$. Then, $P_{\text{out},2}^{\text{TCAP},\infty}$ is obtained as

$$\begin{aligned}P_{\text{out},2}^{\text{TCAP},\infty}&=\frac{2\omega_0R^{\alpha L}\Theta_{p,2}^L}{L!\left(\alpha L+2\right)\left(\delta\tau_2\right)^L}+\frac{2\omega_LR^{\alpha L}\Theta_{c,2}^L}{L!\left(\alpha L+2\right)\delta^L}\\&+\sum_{k=1}^{L-1}\omega_k\left(1-P_{\text{CP},2,k}^{\text{TCAP},\infty}\right).\end{aligned} \tag{74}$$

For $\rho\to\infty$, we have $b_2\to0$ and $b_3\to0$. Thus, for $0<k<L$, when $b_1=1$, based on (50), the $P_{\text{CP},2,k}^{\text{TCAP},\infty}$ is obtained as

$$\begin{aligned}P_{\text{CP},2,k}^{\text{TCAP},\infty}&=\mathbb{E}_{r_2}\left[\bar{F}_{\mu_{c,2}}^{\infty}\left(b_2r_2^{\alpha}\right)\bar{F}_{v_2}^{\infty}\left(b_3r_2^{\alpha}\right)\right]\\&=1-\frac{2b_2^kR^{\alpha k}}{k!\left(\alpha k+2\right)}+\frac{2b_3^{L-k}R^{\alpha L}}{(L-k)!}\\&\times\left(\frac{b_2^k}{k!\left(\alpha L+2\right)}-\frac{R^{-\alpha k}}{\alpha\left(L-k\right)+2}\right)\\&\approx1-\frac{2b_3^{L-k}R^{\alpha(L-k)}}{(L-k)!\left(\alpha\left(L-k\right)+2\right)}-\frac{2b_2^kR^{\alpha k}}{k!\left(\alpha k+2\right)}.\end{aligned} \tag{75}$$

Finally, by substituting (75) into (74), $P_{\text{out},2}^{\text{TCAP},\infty}$ with $b_1=1$ is obtained as

$$\begin{aligned}P_{\text{out},2}^{\text{TCAP},\infty}&=\frac{2\omega_0R^{\alpha L}\Theta_{p,2}^L}{L!\left(\alpha L+2\right)\left(\delta\tau_2\right)^L}+\frac{2\omega_LR^{\alpha L}\Theta_{c,2}^L}{L!\left(\alpha L+2\right)\delta^L}\\&+\sum_{k=1}^{L-1}\left(\frac{2\omega_kb_2^kR^{\alpha k}}{k!\left(\alpha k+2\right)}+\frac{2\omega_kb_3^{L-k}R^{\alpha(L-k)}}{(L-k)!\left(\alpha\left(L-k\right)+2\right)}\right)\\&\approx\sum_{k=1}^{L-1}\left(\frac{2\omega_kb_2^kR^{\alpha k}}{k!\left(\alpha k+2\right)}+\frac{2\omega_kb_3^{L-k}R^{\alpha(L-k)}}{(L-k)!\left(\alpha\left(L-k\right)+2\right)}\right)\\&\approx\frac{2\left(\omega_1b_2+\omega_{L-1}b_3\right)R^{\alpha}}{\alpha+2}.\end{aligned} \tag{76}$$

For $b_1<1$, based on (51), we have $P_{\text{CP},2,k}^{\text{TCAP},\infty}=I_3^{\infty}-I_4^{\infty}$, where I_3^{∞} is obtained as

$$\begin{aligned}I_3^{\infty}&=\mathbb{E}_{r_2}\left[\int_{b_7r_2^{\alpha}}^{\infty}F_{v_2}^{\infty}\left(b_5y-b_6r_2^{\alpha}\right)f_{\mu_{c,2}}\left(y\right)dy\right]\\&=\mathbb{E}_{r_2}\left[1-\frac{b_7^kr_2^{\alpha k}}{k!}\right]\\&-\mathbb{E}_{r_2}\left[\sum_{t=0}^{L-k-1}\frac{b_5^t(b_5+1)^{-t-k}}{(k-1)!t!}\Gamma\left(t+k,\left(b_5+1\right)b_7r_2^{\alpha}\right)\right]\\&\approx1-\frac{b_7^k}{k!}\mathbb{E}_{r_2}\left[r_2^{\alpha k}\right]-\sum_{t=0}^{L-k-1}\frac{b_5^t\left(t+k-1\right)!}{\left(b_5+1\right)^{t+k}\left(k-1\right)!t!}\\&+\sum_{t=0}^{L-k-1}\frac{b_5^tb_7^{t+k}}{(k-1)!t!\left(t+k\right)}\mathbb{E}_{r_2}\left[r_2^{\alpha(t+k)}\right]\\&\approx1-\sum_{t=0}^{L-k-1}\frac{b_5^t\left(t+k-1\right)!}{t!\left(k-1\right)!(b_5+1)^{t+k}}.\end{aligned} \tag{77}$$

Utilizing the same method as I_3^{∞}, and utilizing $F_X\left(x\right)=\frac{x^{\kappa_X}}{\kappa_X!}+\mathcal{O}\left(x^{\kappa_X}\right)$, I_4^{∞} is obtained as

$$\begin{aligned}I_4^{\infty}&=\mathbb{E}_{r_2}\left[F_{v_2}^{\infty}\left(b_3r_2^{\alpha}\right)\bar{F}_{\mu_{c,2}}^{\infty}\left(b_7r_2^{\alpha}\right)\right]\\&=\frac{b_3^{L-k}}{(L-k)!}\mathbb{E}_{r_2}\left[r_2^{\alpha(L-k)}\right]\\&-\frac{b_3^{L-k}b_7^k}{(L-k)!k!}\mathbb{E}_{r_2}\left[r_2^{\alpha L}\right]\\&=\frac{2b_3^{L-k}R^{\alpha L}}{(L-k)!}\left(\frac{R^{-\alpha k}}{\alpha\left(L-k\right)+2}-\frac{b_7^k}{\left(\alpha L+2\right)k!}\right)\\&\approx\frac{2b_3^{L-k}R^{\alpha(L-k)}}{(L-k)!\left(\alpha\left(L-k\right)+2\right)}.\end{aligned} \tag{78}$$

Then, $P_{\mathrm{out},2}^{\mathrm{TCAP},\infty}$ with $b_1 < 1$ is obtained as

$$\begin{aligned} P_{\mathrm{out},2}^{\mathrm{TCAP},\infty} &= \frac{2\omega_0 R^{\alpha L}\Theta_{p,2}^{L}}{L!\left(\alpha L+2\right)\left(\delta\tau_2\right)^{L}} + \frac{2\omega_L R^{\alpha L}\Theta_{c,2}^{L}}{L!\left(\alpha L+2\right)\delta^{L}} \\ &+ \sum_{k=1}^{L-1}\frac{2\omega_k b_3^{L-k}R^{\alpha(L-k)}}{(L-k)!\left(\alpha\left(L-k\right)+2\right)} \\ &+ \sum_{k=1}^{L-1}\sum_{t=0}^{L-k-1}\frac{\omega_k b_5^{t}\left(t+k-1\right)!}{(k-1)!t!(b_5+1)^{t+k}} \\ &\approx \sum_{k=1}^{L-1}\sum_{t=0}^{L-k-1}\frac{\omega_k b_5^{t}\left(t+k-1\right)!}{(k-1)!t!(b_5+1)^{t+k}}. \end{aligned} \tag{79}$$

Similarly when $b_1 > 1$ and $b_7 > 0$, based on (55)- (57), utilizing $\Upsilon\left(n,x\right) \overset{x\to 0}{\approx} \frac{x^n}{n}$, $P_{\mathrm{CP},2,k}^{\mathrm{TCAP},\infty}$ is obtained as

$$\begin{aligned} P_{\mathrm{CP},2,k}^{\mathrm{TCAP},\infty} &= \mathbb{E}_{r_2}\left[\bar{F}_{v_2}^{\infty}\left(b_3 r_2^{\alpha}\right)\bar{F}_{\mu_{c,2}}^{\infty}\left(b_7 r_2^{\alpha}\right)\right] \\ &+ \mathbb{E}_{r_2}\left[\int_0^{b_7 r_2^{\alpha}}\left(1-F_{v_2}^{\infty}\left(b_5 y - b_6 r_2^{\alpha}\right)\right)f_{\mu_{c,2}}\left(y\right)dy\right] \\ &= 1 + \frac{2b_3^{L-k}R^{\alpha L}}{(L-k)!}\left(\frac{b_7^{k}}{\left(\alpha L+2\right)k!} - \frac{R^{-\alpha k}}{\alpha\left(L-k\right)+2}\right) \\ &- \frac{2b_7^{k}R^{\alpha k}}{\left(\alpha k+2\right)k!} + \sum_{t=0}^{L-k-1}\frac{2b_5^{t}b_7^{t+k}R^{\alpha(t+k)}}{t!\left(k-1\right)!\left(t+k\right)\left(\alpha\left(t+k\right)+2\right)} \\ &\approx 1 - \frac{2b_3^{L-k}R^{\alpha(L-k)}}{(L-k)!\left(\alpha\left(L-k\right)+2\right)}. \end{aligned} \tag{80}$$

When $b_1 > 1$ and $b_7 \leq 0$, based on (59), $P_{\mathrm{CP},2,k}^{\mathrm{TCAP},\infty}$ is obtained as

$$\begin{aligned} P_{\mathrm{CP},2,k}^{\mathrm{TCAP},\infty} &= \mathbb{E}_{r_2}\left[\bar{F}_{v_2}^{\infty}\left(b_3 r_2^{\alpha}\right)\right] \\ &= 1 - \frac{b_3^{L-k}}{(L-k)!}\mathbb{E}_{r_2}\left[r_2^{\alpha(L-k)}\right] \\ &= 1 - \frac{2b_3^{L-k}R^{\alpha(L-k)}}{(L-k)!\left(\alpha\left(L-k\right)+2\right)}. \end{aligned} \tag{81}$$

Subsequently, $P_{\mathrm{CP},2,k}^{\mathrm{TCAP},\infty}$ with $b_1 > 1$ is obtained as

$$P_{\mathrm{CP},2,k}^{\mathrm{TCAP},\infty} = 1 - \frac{2b_3^{L-k}R^{\alpha(L-k)}}{(L-k)!\left(\alpha\left(L-k\right)+2\right)}. \tag{82}$$

Finally, by substituting (82) into (74), $P_{\mathrm{out},2}^{\mathrm{TCAP},\infty}$ for $b_1 > 1$ is obtained as

$$\begin{aligned} P_{\mathrm{out},2}^{\mathrm{TCAP},\infty} &= \frac{2\omega_0 R^{\alpha L}\Theta_{p,2}^{L}}{L!\left(\alpha L+2\right)\left(\delta\tau_2\right)^{L}} + \frac{2\omega_L R^{\alpha L}\Theta_{c,2}^{L}}{L!\left(\alpha L+2\right)\delta^{L}} \\ &+ \sum_{k=1}^{L-1}\frac{2\omega_k b_3^{L-k}R^{\alpha(L-k)}}{(L-k)!\left(\alpha\left(L-k\right)+2\right)} \\ &\approx \sum_{k=1}^{L-1}\frac{2\omega_k b_3^{L-k}R^{\alpha(L-k)}}{(L-k)!\left(\alpha\left(L-k\right)+2\right)} \approx \frac{2\omega_{L-1}b_3 R^{\alpha}}{\alpha+2}. \end{aligned} \tag{83}$$

References

[1] M. Xiao, S. Mumtaz, Y. Huang, L. Dai, Y. Li, M. Matthaiou, G. K. Karagiannidis, E. Björnson, K. Yang, I. C. -L, and A. Ghosh, "Millimeter wave communications for future mobile networks," *IEEE J. Sel. Areas Commun.*, vol. 35, no. 9, pp. 1909-1935, Sep. 2017.

[2] S. He, Y. Zhang, J. Wang, J. Zhang, J. Ren, Y. Zhang, W. Zhuang, and X. Shen, "A survey of millimeter-wave communication: physical-layer technology specifications and enabling transmission technologies," *Proc. IEEE*, vol. 109, no. 10, pp. 1666-1705, Oct. 2021.

[3] A. Alkhateeb, O. El Ayach, G. Leus, and R. W. Heath, "Channel estimation and hybrid precoding for millimeter wave cellular systems," *IEEE J. Sel. Topics Signal Process.*, vol. 8, no. 5, pp. 831-846, Oct. 2014.

[4] Z. Ding, P. Fan, and H. V. Poor, "Random beamforming in millimeter-wave NOMA networks," *IEEE Access*, vol. 5, pp. 7667-7681, Jun. 2017.

[5] X. Sun, W. Yang, and Y. Cai, "Secure communication in NOMA assisted millimeter wave SWIPT UAV networks," *IEEE Internet Things J.*, vol. 7, no. 3, pp. 1884-1897, Mar. 2020.

[6] Y. Cao, S. Wang, M. Jin, N. Zhao, Y. Chen, Z. Ding, and X. Wang, "Joint user grouping and power optimization for secure mmWave-NOMA system," *IEEE Trans. Wireless Commun.*, vol. 21, no. 5, pp. 3307-3320, May 2022.

[7] Y. Ju, H.-M. Wang, T.-X. Zheng, and Q. Yin, "Secure transmissions in millimeter wave systems," *IEEE Trans. Commun.*, vol. 65, no. 5, pp. 2114-2127, May 2017.

[8] Y. Ju, H.-M. Wang, T.-X. Zheng, Q. Yin, and M. H. Lee, "Safeguarding millimeter wave communications against randomly located eavesdroppers," *IEEE Trans. Wireless Commun.*, vol. 17, no. 4, pp. 2675-2689, Apr. 2018.

[9] Y. Ju, H. Wang, Q. Pei, and H.-M. Wang, "Physical layer security in millimeter wave DF relay systems," *IEEE Trans. Wireless Commun.*, vol. 18, no. 12, pp. 5719-5733, Dec. 2019.

[10] S. Huang, M. Xiao, and H. V. Poor, "On the physical layer security of millimeter wave NOMA networks," *IEEE Trans. Veh. Technol.*, vol. 69, no. 10, pp. 11697-11711, Oct. 2020.

[11] Y. Mao, B. Clerckx, and V. O. K. Li, "Rate-splitting multiple access for downlink communication systems: bridging, generalizing, and outperforming SDMA and NOMA," *EURASIP J Wirel Commun Netw*, vol. 2018, no. 1, pp. 1-54, Apr. 2018.

[12] B. Clerckx, Y. Mao, R. Schober, and H. V. Poor, "Rate-splitting unifying SDMA, OMA, NOMA, and multicasting in MISO broadcast channel: A simple two-user rate analysis," *IEEE Wireless Commun. Lett.*, vol. 9, no. 3, pp. 349-353, Mar. 2020.

[13] Y. Mao, B. Clerckx, and V. O. K. Li, "Rate-splitting for multi-antenna non-orthogonal unicast and multicast transmission: Spectral and energy efficiency analysis," *IEEE Trans. Commun.*, vol. 67, no. 12, pp. 8754-8770, Dec. 2019.

[14] Y. Mao, O. Dizdar, B. Clerckx, R. Schober, P. Popovski, and H. V. Poor, "Rate-splitting multiple access: Fundamentals, survey, and future research trends," *IEEE Commun. Surveys Tuts.*, vol. 24, no. 4, pp. 2073-2126, 4th Quart. 2022.

[15] H. Joudeh and B. Clerckx, "Rate-splitting for max-min fair multigroup multicast beamforming in overloaded systems," *IEEE Trans. Wireless Commun.*, vol. 16, no. 11, pp. 7276-7289, Nov. 2017.

[16] S. K. Singh, K. Agrawal, K. Singh, and C.-P. Li, "Outage probability and throughput analysis of UAV-assisted rate-splitting multiple access," *IEEE Wireless Commun. Lett.*, vol. 10, no. 11, pp. 2528-2532, Nov. 2021.

[17] Z. Lin, M. Lin, T. de Cola, J.-B. Wang, W.-P. Zhu, and J. Cheng, "Supporting IoT with rate-splitting multiple access in satellite and aerial-integrated networks," *IEEE Internet Things J.*, vol. 8, no. 14, pp. 11123-11134, Jul. 2021.

[18] M. Abolpour, S. Aissa, L. Musavian, and A. Bhowal, "Rate splitting in the presence of untrusted users: Outage and secrecy outage performances," *IEEE Open J. Commun. Soc.*, vol. 3, pp. 921-935, Jun. 2022.

[19] Y. Tong, D. Li, Z. Yang, Z. Xiong, N. Zhao, and Y. Li, "Outage analysis of rate splitting networks with an untrusted user," in *IEEE Trans. Veh. Technol.*, doi: 10.1109/tvt.2022.3209794, 2022

[20] Q. Zhu, Z. Qian, B. Clerckx, and X. Wang. "Rate-splitting multiple access in multi-cell dense networks: A stochastic geometry approach," *arXiv:2207.11430*, Jul. 2022, [Online]: https://arxiv.org/abs/2207.11430.

[21] B. Rimoldi and R. Urbanke, "A rate splitting approach to the gaussian multiple-access channel," *IEEE Trans. Inf. Theory*, vol. 42, no. 2, pp. 364-375, Mar. 1996.

[22] H. Liu, T. A. Tsiftsis, K. J. Kim, K. S. Kwak, and H. V. Poor, "Rate splitting for uplink NOMA with enhanced fairness and outage performance," *IEEE Trans. Wireless Commun.*, vol. 19, no. 7, pp. 4657-4670, Jul. 2020.

[23] H. Liu, Z. Bai, H. Lei, G. Pan, K. J. Kim, and T. A. Tsiftsis, "A new rate splitting strategy for uplink CR-NOMA systems," *IEEE Trans. Veh. Technol.*, vol. 71, no. 7, pp. 7947-7951, Jul. 2022.

[24] S. A. Tegos, P. D. Diamantoulakis, and G. K. Karagiannidis, "On the performance of uplink rate-splitting multiple access," *IEEE Commun. Lett.*, vol. 26, no. 3, pp. 523-527, Mar. 2022.

[25] B. Clerckx, Y. Mao, R. Schober, E. A. Jorswieck, D. J. Love, J. Yuan, L. Hanzo, G. Y. Li, E. G. Larsson, and G. Caire, "Is NOMA efficient in multi-antenna networks? A critical look at next generation multiple

access techniques," *IEEE Open J. Commun. Soc.*, vol. 2, pp. 1310-1343, Jun. 2021.

[26] M. Dai and B. Clerckx, "Multiuser millimeter wave beamforming strategies with quantized and statistical CSIT," *IEEE Trans. Wireless Commun.*, vol. 16, no. 11, pp. 7025-7038, Nov. 2017.

[27] B. Clerckx, H. Joudeh, C. Hao, M. Dai, and B. Rassouli, "Rate splitting for MIMO wireless networks: A promising PHY-layer strategy for LTE evolution," *IEEE Commun. Mag.*, vol. 54, no. 5, pp. 98-105, May 2016.

[28] H. Joudeh and B. Clerckx, "Sum-rate maximization for linearly precoded downlink multiuser MISO systems with partial CSIT: A rate-splitting approach," *IEEE Trans. Commun.*, vol. 64, no. 11, pp. 4847-4861, NOV. 2016.

[29] T. S. Rappaport, Y. Xing, G. R. MacCartney, A. F. Molisch, E. Mellios, and J. Zhang, "Overview of millimeter wave communications for fifth-generation (5G) wireless networks—with a focus on propagation models," *IEEE. T. Antenn. Propag*, vol. 65, no. 12, pp. 6213-6230, Dec. 2017.

[30] A. Alkhateeb, G. Leus, and J. Robert W. Heath, "Limited feedback hybrid precoding for multi-user millimeter wave systems," *IEEE Trans. Wireless Commun.*, vol. 14, no. 11, pp. 6481-6494, Nov. 2015.

[31] I. S. Gradshteyn and I. M. Ryzhik, *Table of Integrals, Series, and Products*, 7th edition. Academic Press, 2007.

[32] C. Wang and H.-M. Wang, "Physical layer security in millimeter wave cellular networks," *IEEE Trans. Wireless Commun.*, vol. 15, no. 8, pp. 5569-5585, Aug. 2016.

[33] Y. Zhu, L. Wang, K. K. Wong, and R. W. Heath, "Secure communications in millimeter wave ad hoc networks," *IEEE Trans. Wireless Commun.*, vol. 16, no. 5, pp. 3205-3217, May 2017.

Hongjiang Lei (Senior Member, IEEE) received the B.Sc. degree in Mechanical and Electrical Engineering from Shenyang Institute of Aeronautical Engineering, Shenyang, China, in 1998, the M.Sc. degree in Computer Application Technology from Southwest Jiaotong University, Chengdu, China, in 2004, and the Ph.D. degree in Instrument Science and Technology from Chongqing University, Chongqing, China, in 2015, respectively. From November 2016 to October 2018, he was a Postdoctoral Research Fellow with CEMSE Division, King Abdullah University of Science and Technology (KAUST), Saudi Arabia. In May 2004, he joined the School of Communication and Information Engineering of Chongqing University of Posts and Telecommunications (CQUPT), Chongqing, China, where he is currently a Full Professor. His current research interests include physical layer security and performance analysis of wireless communication systems.

Sha Zhou received the B.Sc. degree in Electronic and Information Engineering from University of South China, Hunan, China, in 2020. She is currently pursuing the M.Sc. degree in Information and Communication Engineering at Chongqing University of Posts and Telecommunications (CQUPT), Chongqing, China. Her research interests include performance analysis of wireless communication systems and millimeter wave communications.

Ki-Hong Park (Senior Member, IEEE) received the B.Sc. degree in electrical, electronic, and radio engineering from Korea University, Seoul, Korea, in 2005 and the M.S. and Ph.D. degrees from the School of Electrical Engineering, Korea University, Seoul, Korea, in 2011. Since April 2011, he has been a Postdoctoral Fellow of Electrical Engineering in the Division of Physical Science and Engineering, King Abdullah University of Science and Technology (KAUST), Thuwal, Saudi Arabia. His research interests are broad in communication theory and its application to the design and performance evaluation of wireless communication systems and networks. On-going research includes the application to MIMO diversity/beamforming systems, cooperative relaying systems, physical layer secrecy, and optical wireless communications.

Imran Shafique Ansari (Member, IEEE) received the B.Sc. degree in Computer Engineering from King Fahd University of Petroleum and Minerals (KFUPM) in 2009 (with First Honors) and M.Sc. and PhD degrees from King Abdullah University of Science and Technology (KAUST) in 2010 and 2015, respectively. Since August 2018, he is a Lecturer (Assistant Professor) with University of Glasgow, Glasgow, UK. Prior to this, from November 2017 to July 2018, he was a Lecturer (Assistant Professor) with Global College of Engineering and Technology (GCET) (affiliated with University of the West of England (UWE), Bristol, UK). From April 2015 to November 2017, he was a Postdoctoral Research Associate (PRA) with Texas A&M University at Qatar (TAMUQ). From May 2009 through Aug. 2009, he was a visiting scholar with Michigan State University (MSU), East Lansing, MI, USA, and from Jun. 2010 through Aug. 2010, he was a research intern with Carleton University, Ottawa, ON, Canada. His current research interests include free-space optics (FSO), channel modeling/signal propagation issues, relay/multihop communications, physical layer security, full duplex systems, and secure D2D applications for 5G+ systems, among others.

Hong Tang received his B.Sc. degree in Optics and M.Sc. degree in Optics from Sichuan University, Chengdu, China, in 1990 and 1995, and Ph. D. degree in Computer Software and Theory from Chongqing University, Chongqing, China, in 2003. He is now a professor in School of Communication and Information Engineering, CQUPT. His research focuses on wireless communications technology, including big data and blockchain technology.

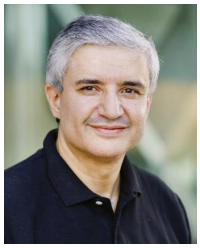

Mohamed-Slim Alouini (Fellow IEEE) was born in Tunis, Tunisia. He received the Ph.D. degree in Electrical Engineering from the California Institute of Technology (Caltech), Pasadena, CA, USA, in 1998. He served as a faculty member in the University of Minnesota, Minneapolis, MN, USA, then in the Texas A&M University at Qatar, Education City, Doha, Qatar before joining King Abdullah University of Science and Technology (KAUST), Thuwal, Makkah Province, Saudi Arabia as a Professor of Electrical Engineering in 2009. His current research interests include the modeling, design, and performance analysis of wireless communication systems.